RESEARCH ARTICLE

Design of Adaptive Constellations and Error Protection Coding for Wireless Network Coding in 5-node Butterfly Networks

Pavel Prochazka[1], Tomas Uricar[1], David Halls[2*] and Jan Sykora[1]

*Correspondence:

david.halls@toshiba-trel.com

[2]Toshiba – Telecommunication
Research Laboratory, 32 Queen
Square, BS1 4ND Bristol,, UK
Full list of author information is
available at the end of the article

Abstract

In this paper we focus on the design of a reliable communication scheme for generic 5-node Wireless Butterfly Networks (WBN). Since the WBN represents a natural extension of the basic 2-way relay communication channel, we follow the paradigm of *Wireless Physical Layer Network Coding* and we show that the design of novel adaptive constellations is desirable to exploit the promising performance of wireless network coding in WBN. We introduce a *systematic constellation design* algorithm and we show that the proposed constellations are capable of outperforming conventional point-to-point modulations in WBN over the whole range of channel signal to noise ratios. To further support the applicability of the proposed constellations in a practical system, we integrate a simple binary channel coding scheme, providing a robust *adaptive modulation and coding scheme* for relaying in symmetric WBNs with arbitrary channel conditions.

Keywords: wireless network coding; butterfly network; relaying; superposition coding; superposition modulation

1 Introduction

The invention of Wireless Network Coding (WNC) has indeed provided a means for a significant enhancement in wireless system performance [1–3]. However, WNC processing

Figure 1 Symmetric WBN model with half-duplex constraint and 2-phase communication.
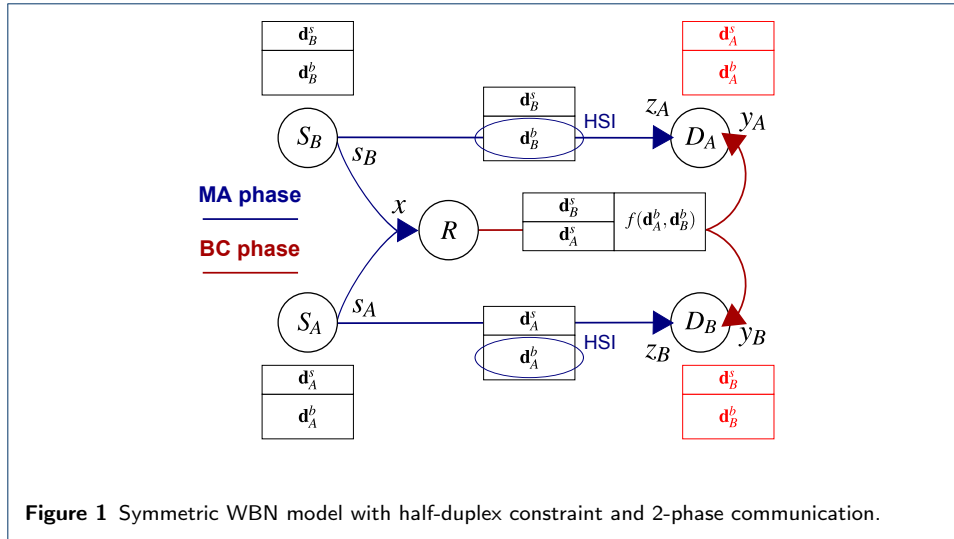
has also revealed several non-trivial research problems which do not have counterparts in conventional point-to-point or multi-user systems, like the sensitivity to channel parameterization [4–7] or challenging multi-source transmission synchronization [8–10]. Furthermore, the specific characteristics of multi-node WNC systems can call also for novel constellation design approaches (see e.g. [7, 11]).

In WNC the transmitted information symbols are allowed to interact directly in the constellation space, inducing a specific set of requirements on the constellations' properties and characteristics (see e.g. [7, 11]). Generally we can declare [11] that any constellation suitable for the specific nature of WNC processing should be able to form *a superimposed constellation* with an appropriate structure at all receiving nodes (allowing direct decoding of specific WNC functions of user data from the received non-orthogonal signals [12, 13]) and simultaneously it should be able to exploit the *broadcast nature* of wireless channels (allowing a reduction in the consumption of channel resources in the system [1]). Since both of these properties hinge on the actual SNR conditions in the system, the constellation design itself can become a relatively challenging task.

One of the first attempts to design a suitable multi-source constellation for communication in a multi-node WNC system was introduced in our previous work [11], where the *adaptive 2-source constellations* for WNC-based communication in a 5-node *Wireless But-*

terfly Network (WBN) were developed. However, the results presented in [11] are limited to an uncoded system, which significantly limits its practical applicability.

In this paper we extend the communication scheme from [11] by appending appropriate *error protection coding* to the system, resulting in a practical channel-coded adaptive communication scheme for WBN. We provide the following results and contributions:

1   We summarize the *systematic constellation design algorithm* from [11] and we provide additional numerical results analysing its promising performance.

2   We revise and extend the results discussing the *adaptive capabilities of the constellations,* including *the constellation mapping regions* for adaptive WBN relaying.

3   We validate the proposed design in a *real-world HW setup*, including the HW evaluation of adaptive system performance.

4   We show how the *channel coding* can be integrated into the proposed constellation design, including the analysis of proper source transmission rates.

5   We evaluate numerically the performance of the resulting *adaptive modulation and coding* scheme for a wide range of channel conditions in the WBN.

6   We show that the proposed design is viable even if the real-world conditions induce some deviation from the assumed system model.

The rest of the paper is organized as follows. The system model, including all necessary definitions and details about WNC processing in WBNs is summarized in Section 2. A systematic *constellation design algorithm* for WBNs is revised in Section 3. The performance analysis of the proposed constellations (including the HW evaluation) in an uncoded system is available in Section 4. Section 5 discusses an adaptive constellation design and Section 6 introduces the channel coding extension to the system. The performance of the novel adaptive modulation and coding scheme is analyzed in Section 7, including a simple robustness analyzis. Concluding remarks are summarized in Section 8.

2 WNC Relaying in Wireless Butterfly Network

We assume a *symmetric* WBN model [14, 15] with a half-duplex constraint (Fig. 1). An example practical scenario complying with the WBN model is a communication among vehicles and road-side infrastructure nodes for traffic information exchange on a bidirectional highway within two time slots [16]. The direct channels between the intended source→destination pairs are not available in WBN and thus the help of the intermediate relay node is necessary to enable end-to-end communication. Note that some partial source material from the implementation of this model can be found in [17].

2.1 Relaying Strategy

An information-theoretic relaying strategy (based on Superposition Coding (SC) [18–21]) for WBNs was proposed in [14, 15]. The fundamental idea of the SC-approach is to split each data symbol $\mathbf{d}_i$ at source $i \in \{A, B\}$ into the *basic part* $\mathbf{d}_i^b = [d_{i,0}^b, \ldots, d_{i,N_b-1}^b]$ and the *superposed part* $\mathbf{d}_i^s = [d_{i,0}^s, \ldots, d_{i,N_s-1}^s]$, $d_{i,n}^b, d_{i,n}^s \in \{0, 1\}$, and then process each of the resulting data streams separately throughout the system (see Fig. 1). While the basic part represents a "true WNC" information stream (limited by the amount of available HSI) in the system, the superposed part defines the "routed" information which is appended on top of the WNC stream to exploit any potential spare capacity of related channels in the system (see [14, 15] for more details). A simplified description of SC-based relaying in an uncoded WBN system is summarized in Table 1 and depicted in Fig. 2.

2.2 System Model

For the sake of simplicity of the constellation design analysis, we provisionally assume that the system is uncoded[1]. The signal space representations of the transmitted channel symbols are $s_A = \mathscr{A}^A(\mathbf{d}_A)$, $s_B = \mathscr{A}^B(\mathbf{d}_B)$, where $\mathscr{A}^i(\cdot)$ is the memoryless constellation mapper and $\mathbf{d}_i$ is the source $i \in \{A, B\}$ data symbol. Each communication round can be divided into two phases (Fig. 1). In the first phase (Multiple Access – MA phase) both

---

[1]Modification of the system model for the coded case will be provided in Section 6, together with a discussion on the design of individual channel encoders for particular information streams in the system.

Step 1: Source transmission

- Source S_i, $i \in \{A, B\}$ maps its data symbol $\mathbf{d}_i = \left[\mathbf{d}_i^b; \mathbf{d}_i^s\right]$ into a $(N_b + N_s)$-bit superposition modulation symbol

$$s_i = \mathscr{A}^i \left(\left[\mathbf{d}_i^b; \mathbf{d}_i^s\right] \right), \tag{1}$$

- S_A, S_B simultaneously transmit their signals to the relay and unintended destinations (Fig. 1).
- Relay receives

$$x = h_{AR} \mathscr{A}^A \left(\left[\mathbf{d}_A^b; \mathbf{d}_A^s\right] \right) + h_{BR} \mathscr{A}^B \left(\left[\mathbf{d}_B^b; \mathbf{d}_B^s\right] \right) + w_R \tag{2}$$

and decodes $\left[\mathbf{d}_A^s; \mathbf{d}_B^s; f(\mathbf{d}_A^b, \mathbf{d}_B^b)\right]$, where f is a hierarchical WNC function [13].

- D_j receives

$$z_j = h_{ij} \mathscr{A}^i \left(\left[\mathbf{d}_i^b; \mathbf{d}_i^s\right] \right) + w_j, \tag{3}$$

where $i, j \in \{A, B\}$, $i \neq j$ and stores the signal for further processing.
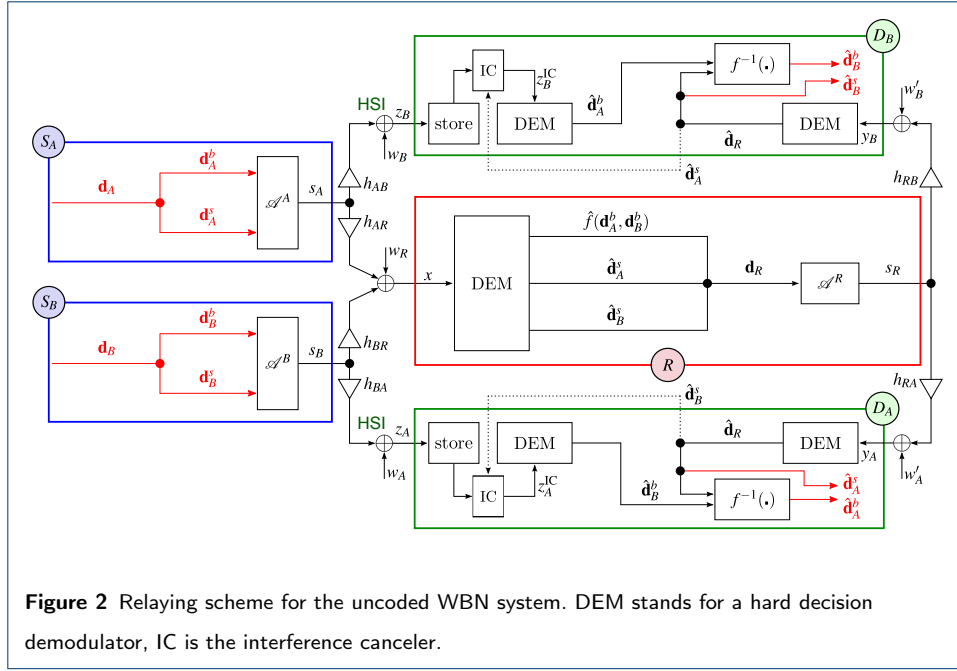
Step 2: Relay broadcast

- Relay sends $N_R = 2N_s + N_b$-bit modulation symbol to both destinations:

$$s_R = \mathscr{A}^R \left(\left[\mathbf{d}_A^s; \mathbf{d}_B^s; f(\mathbf{d}_A^b, \mathbf{d}_B^b)\right] \right). \tag{4}$$

- D_j ($i, j \in \{A, B\}$, $i \neq j$) decodes:
    - $\left[\mathbf{d}_A^s; \mathbf{d}_B^s; f(\mathbf{d}_A^b, \mathbf{d}_B^b)\right]$ (from the relay signal (4))
    - $\mathbf{d}_i^b$ (from the stored signal z_j (3), after interference cancellation (IC) of known $\mathbf{d}_i^s$)
    - $\mathbf{d}_j^b$ (from $\mathbf{d}_i^b$ and $f(\mathbf{d}_A^b, \mathbf{d}_B^b)$, using a standard WNC decoding [13])
- D_j merges $\mathbf{d}_j^b$ with $\mathbf{d}_j^s$ to obtain the desired $\left[\mathbf{d}_j^b; \mathbf{d}_j^s\right]$.

Table 1 SC-based relaying scheme in uncoded WBN

.

Figure 2 Relaying scheme for the uncoded WBN system. DEM stands for a hard decision demodulator, IC is the interference canceler.

sources S_A, S_B simultaneously transmit their signal to the relay, which receives a noisy superimposed constellation:

$$x = h_{AR}s_A + h_{BR}s_B + w_R. \tag{5}$$

Additionally, the source S_i ($i \in \{A,B\}$) transmission is overheard (at no cost) by its "unintended" destination D_j ($j \in \{A,B\}$, $j \neq i$) as:

$$z_j = h_{ij}s_i + w_j \tag{6}$$

Even though the overheard information (6) does not carry the desired data for the respective destination, it can be efficiently exploited to enable WNC-based processing in WBNs [14]. We denote the specific overheard information as the *Hierarchical Side Information* (HSI) [15].

The relay performs WNC-based decoding [13] of the received signal and broadcasts the decoded WNC (hierarchical) information as s_R to D_A, D_B in the second phase (Broadcast

– BC phase). Both destinations are able to decode the desired data using the relay's (hierarchical) signal (5) and the overheard HSI (6) if a proper WNC processing is employed in the system.

Scalar complex channel coefficients h_{ij}, $i,j \in \{A,B,R\}$, $i \neq j$ are assumed to be constant during the communication round and known at the respective receiving node. Zero mean i.i.d. complex Gaussian noise sample w_i, $i \in \{A,B,R\}$ has variance σ_i^2. Signal to Noise Ratios (SNRs) in the system are given by (γ_{MAC}, γ_{HSI}, γ_{BC}), where γ_{MAC} is the SNR on the source→relay multiple-access channel – MAC (($S_A, S_B) \to R$), γ_{HSI} is the SNR on the unintended source→destination (HSI) channels ($S_A \to D_B$, $S_B \to D_A$) and γ_{BC} is the SNR on the relay→sources broadcast channel ($R \to (D_A, D_B)$).

3 Superposition Modulation Design

In this section we summarize the design of constellation mappers $\mathscr{A}^A$, $\mathscr{A}^B$ as presented in [11]. The output constellation is created as

$$s = \mathscr{A}\left(\left[\mathbf{d}^b; \mathbf{d}^s\right]\right) = \sum_{n_s=0}^{N_s-1} L_{n_s}^s (2d_{n_s}^s - 1) + \sum_{n_b=0}^{N_b-1} L_{n_b}^b (2d_{n_b}^b - 1), \tag{7}$$

where L_n^b, L_n^s are *Superposition Modulation* [22] *scaling coefficients.*

The coefficients L_n^b, L_n^s (7) are generally taken from the set of complex numbers. However, for the sake of simplicity we limit the scaling coefficients L_n^b, L_n^s to a purely imaginary or real numbers. Even though that this simplified approach can potentially result in a suboptimal performance in fading channels (complex channel coefficients h_{iR}, $i \in \{A,B\}$ can rotate the component superposition constellations), we follow this simplification to show the basic ideas of the proposed superposition modulation design. The extension to general complex L_n^b, L_n^s can naturally embrace the source phase pre-rotation [23–25], which virtually reverts the fading channel to the conventional Additive White Gaussian Noise (AWGN) channel with $\sphericalangle h_{ij} = 0$.

As shown in Table 1, the basic and superposed parts of the source information are processed in a different way through the system and so we will discuss the constellation design for these two specific information streams separately. We briefly introduce the incentives and main ideas of the design for the superposed and basic parts, and then we summarize the complete multi-source constellation design in a systematic algorithm.

3.1 Constellation Design: Basic part

A specific WNC function $f(\mathbf{d}_A^b, \mathbf{d}_B^b)$ has to be decoded by the relay (Table 1) and hence some overlapping of symbols in the superimposed constellation (observed by the relay node) can be allowed, resulting in improved Euclidean distance properties. More precisely, two (or more) pairs of basic information symbols $(\mathbf{d}_A^b, \mathbf{d}_B^b)$, $\left(\mathbf{d'}_A^b, \mathbf{d'}_B^b\right)$ can be allowed to fall into the same point in the superimposed constellation:

$$s_A\left(\mathbf{d}_A^b\right) + s_B\left(\mathbf{d}_B^b\right) = s'_A\left(\mathbf{d'}_A^b\right) + s'_B\left(\mathbf{d'}_B^b\right),\tag{8}$$

if and only if they belong to the same WNC function output, i.e. iff $f(\mathbf{d}_A^b, \mathbf{d}_B^b) = f(\mathbf{d'}_A^b, \mathbf{d'}_B^b)$, where $f(\text{\textbf{.}},\text{\textbf{.}})$ is the hierarchical WNC function [13]. In this case the overlapping symbols produce the *same hierarchical output*, which can be successfully resolved by the destination, if matching HSI information is available (Table 1). The particular choice of the scaling coefficients $L_{A,n}^b$, $L_{B,n}^b$ generally depends on the particular choice of the hierarchical WNC function[2]. In the rest of this paper we discuss the constellation design for the *bit-wise exclusive-or* WNC function ($f(\mathbf{d}_A^b, \mathbf{d}_B^b) = \mathbf{d}_A^b \oplus \mathbf{d}_B^b$, where $\oplus$ is the bit-wise XOR operation) [3].

Suitable overlapping of constellation symbols at the relay is provided by letting both sources transmit at the same power level, i.e. $L_{A,n}^b = L_{B,n}^b$ [11]. It can be easily shown that if these superposition modulation (7) coefficients are chosen as $L_{A,n}^b = L_{B,n}^b = 3^{\lfloor n/2 \rfloor}$ (for even n) and $L_{A,n}^b = L_{B,n}^b = \mathrm{j}3^{\lfloor n/2 \rfloor}$ (for odd n), the received superimposed constellation at

---

[2]Modulo-sum [11,26,27] and bit-wise exclusive-or (XOR) [3,23] hierarchical functions are commonly discussed in the WNC literature, however, unlike the bit-wise XOR, implementation of channel coding for the Modulo-sum mapping is a standalone research problem and hence it is out of the scope of this paper.

the relay will have overlaps only among those constellation symbols (8) which have the same hierarchical WNC output i.e. $f(\mathbf{d}_A^b, \mathbf{d}_B^b) = f(\mathbf{d'}_A^b, \mathbf{d'}_B^b) = \mathbf{d}_A^b \oplus \mathbf{d}_B^b = \mathbf{d'}_A^b \oplus \mathbf{d'}_B^b$.

3.2 Constellation Design: Superposed part

The superposed information given by $\mathbf{d}_A^s, \mathbf{d}_B^s$ has to be decoded separately by the relay (Table 1), and hence a source constellation avoiding all potential overlaps in the super-imposed constellation (observed by the relay node) is desirable. In an AWGN channel ($h_{AR} = h_{BR} = 1$ in Fig. 1) this can be simply achieved by mapping the information bits to the real-valued Amplitude Shift Keying (ASK) constellation at S_A and purely imaginary-valued ASK constellation at S_B (or vice versa). Hence, in AWGN, the resulting superimposed constellation at the relay will form a regular QAM constellation without any overlapping of constellation symbols. For the assumed superposition modulation (7), this can be easily achieved by setting the coefficients as $L_{A,n}^s = 2^n$ and $L_{B,n}^s = \text{j} \cdot 2^n$.

Algorithm 1 Constellation design for fixed N_b, N_s.

1: **Input:** (N_b, N_s)
2: **for** $n_s \in \{0, \dots, N_s - 1\}$ ▷ "superposed levels"
3:     $L_{A,n_s}^s \leftarrow 2^{n_s}$, $L_{B,n_s}^s \leftarrow \text{j} 2^{n_s}$
4: **end**
5: **for** $n_b \in \{0, \dots, N_b - 1\}$ ▷ "basic levels"
6:     $L_{A,n_b}^b = L_{B,n_b}^b \leftarrow 2^{N_s} \cdot 3^{\lfloor n_b/2 \rfloor}$ for even n_b
7:     $L_{A,n_b}^b = L_{B,n_b}^b \leftarrow \text{j} 2^{N_s} \cdot 3^{\lfloor n_b/2 \rfloor}$ for odd n_b
8: **end**
9: $\alpha^2 = \sum_{n_s=0}^{N_s-1} |L_{i,n_s}^s|^2 + \sum_{n_b=0}^{N_b-1} |L_{i,n_b}^b|^2$ ▷ "norm. coefficient"
10: **for** $i \in \{A, B\}$ and $\forall \mathbf{d}_i = \left[\mathbf{d}_i^b; \mathbf{d}_i^s\right]$, $d_{i,n_b}^b, d_{i,n_s}^s \in \{0,1\}$:
11:     **for** $n_s \in \{0, N_s - 1\}$, $n_b \in \{0, N_b - 1\}$
12:         $s_{i,n_s}^s = L_{i,n_s}^s \left(2 d_{i,n_s}^s - 1\right)$
13:         $s_{i,n_b}^b = L_{i,n_b}^b \left(2 d_{i,n_b}^b - 1\right)$
14:     **end**
15:     $s_i = \mathscr{A}^i \left(\left[\mathbf{d}_i^b; \mathbf{d}_i^s\right]\right) = \alpha^{-1} \left(\sum_{n_s=0}^{N_s-1} s_{i,n_s}^s + \sum_{n_b=0}^{N_b-1} s_{i,n_b}^b\right)$ ▷ "constellation symbols"
16: **end**
17: **Output:** Constellation alphabets $\mathscr{A}^A$, $\mathscr{A}^B$.

3.3 Systematic Constellation Design Algorithm

To accommodate both the basic and superposed information streams into a joint source constellation, the scaling coefficients of basic information streams (L_n^b) must be pre-scaled

by a factor 2^{N_s} to ensure that they lie above the largest scaling coefficient of the superposed part. The basic stream (WNC) is thus preferred over the superposed one (routing) in order to maximize the overall throughput of the system. The systematic constellation design for arbitrary N_b, N_s is summarized in Algorithm 1.

The basic principle of source constellation design is illustrated in Fig. 3 ($N_b = 2, N_s = 1$) and some example sets of source constellations with constant $N_b + N_s = 2$ are depicted in Fig. 4.
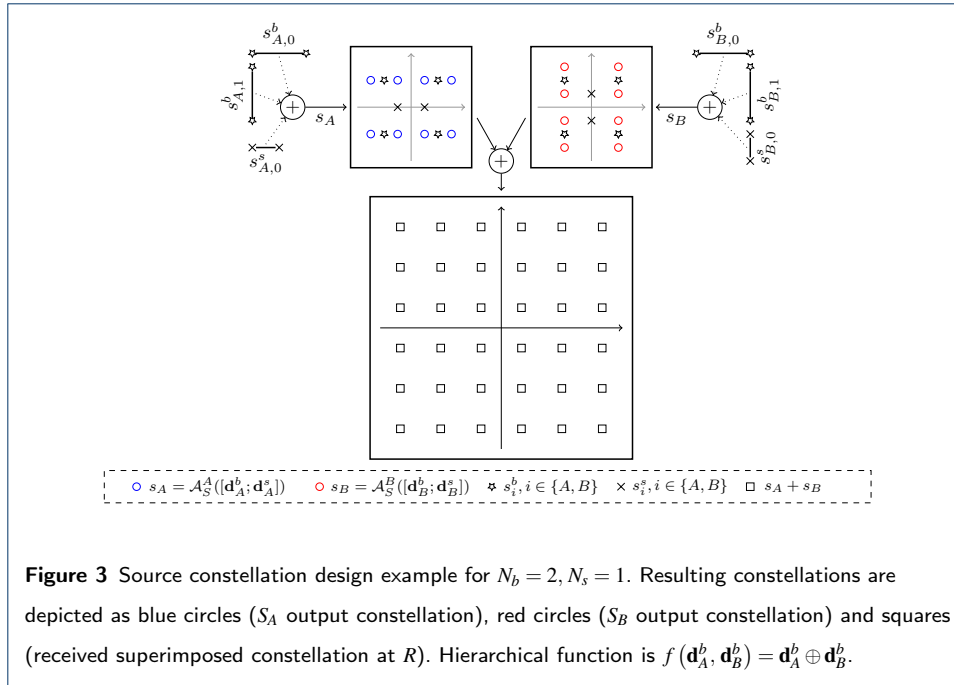
4 Performance Analysis I: Uncoded System

For the sake of simplicity of the theoretical performance analysis, we assume that source→relay channels in WBN are AWGN[3] (i.e. $h_{iR} = 1$ for $i \in \{A, B\}$). We evaluate the throughput analytically as $(N_b + N_s) \cdot (1 - P_e^{\text{FER}})$, where P_e^{FER} denotes the frame error rate. Due to the system symmetry we evaluate the throughput of $S_A \to D_A$ only. We set the frame length to $M = 768$ symbols (to match the HW evaluation) and the relay output mapper $\mathscr{A}^R$ will be defined as a conventional $(2^{N_b + 2N_s})$-QAM constellation. All performance metrics in the symmetric WBN are evaluated as a function of the actual SNRs ($\gamma_{\text{MAC}}, \gamma_{\text{HSI}}, \gamma_{\text{BC}}$).

4.1 Analytical Performance Evaluation

Since all constellations points lie on a regular QAM grid, it is straightforward to evaluate the exact Symbol Error Rate (SER) for all channels analytically. The symbol error probability P_e^{SER} can be approximated by its upper-bound[4] $P_{e,\text{UB}}^{\text{SER}} = 1 - ((1 - P_e^{\text{MAC}})(1 - P_e^{\text{HSI}})(1 - P_e^{\text{BC}}))$, where P_e^{MAC}, P_e^{HSI} and P_e^{BC} are the probabilities of symbol error in the MAC, HSI and BC channels (respectively). Since the system is memoryless, the overall FER is given by $P_e^{\text{FER}} = 1 - (1 - P_e^{\text{SER}})^M$, which can be approximated by $P_{e,\text{UB}}^{\text{FER}} = 1 - (1 - P_{e,\text{UB}}^{\text{SER}})^M$. Nearest neighbor pairwise error approximation can be used for efficient error rate evaluation.

---

[3]Note that this also includes the system with perfect source phase prerotation [23–25], which can be obtained by a generalization of the scaling coefficients as $L'_n = L_n e^{-j\angle h_{SR}}$, where h_{SR} is the corresponding source→relay channel.

[4]The evaluated $P_{e,\text{UB}}^{SER}$ is an upper-bound of P_e^{SER}, since an error in MA/BC phase does not necessarily induce an error in the overall communication chain of the uncoded system. This is especially true if the error occurs in the superposed bits $\mathbf{d}_B^s$ used for interference cancellation processing at D_A.

Figure 3 Source constellation design example for $N_b = 2, N_s = 1$. Resulting constellations are depicted as blue circles (S_A output constellation), red circles (S_B output constellation) and squares (received superimposed constellation at R). Hierarchical function is $f\left(\mathbf{d}_A^b, \mathbf{d}_B^b\right) = \mathbf{d}_A^b \oplus \mathbf{d}_B^b$.

The lower-bound of the throughput can be then evaluated analytically as:

$$T_{\mathrm{LB}} = (N_b + N_s) \cdot (1 - P_{e,\mathrm{UB}}^{\mathrm{FER}}). \tag{9}$$

4.2 Hardware Implementation

In addition to the analytical evaluation of throughput, we validate the results in a real-world setup. The hardware performance is evaluated using Ettus Research Universal Software Radio Peripherals (USRPs) which are computer-hosted Software Defined Radios (SDRs). The USRPs connect to a host computer via a Gigabit Ethernet link, which the host-based software uses to receive and transmit the baseband IQ stream. The host controls the USRP using USRP Hardware Driver (UHD) commands, including setting parameters such as amplifier gain. The USRP then performs the necessary baseband processing then up/down-conversion and transmission/reception. The Ettus Research N210 USRP is used, which consists of a motherboard and a Radio Frequency (RF) daughterboard; more details can be found in [28]. In these experiments the XCVR2450 daughterboards are used, these are dual-band transceivers with 100 mW output at 2.4 - 2.5 GHz and 50 mW output at 4.9 -

Figure 4 Proposed constellation design for $(N_b, N_s) = \{(2,0)\,;(1,1)\,;(0,2)\}$.
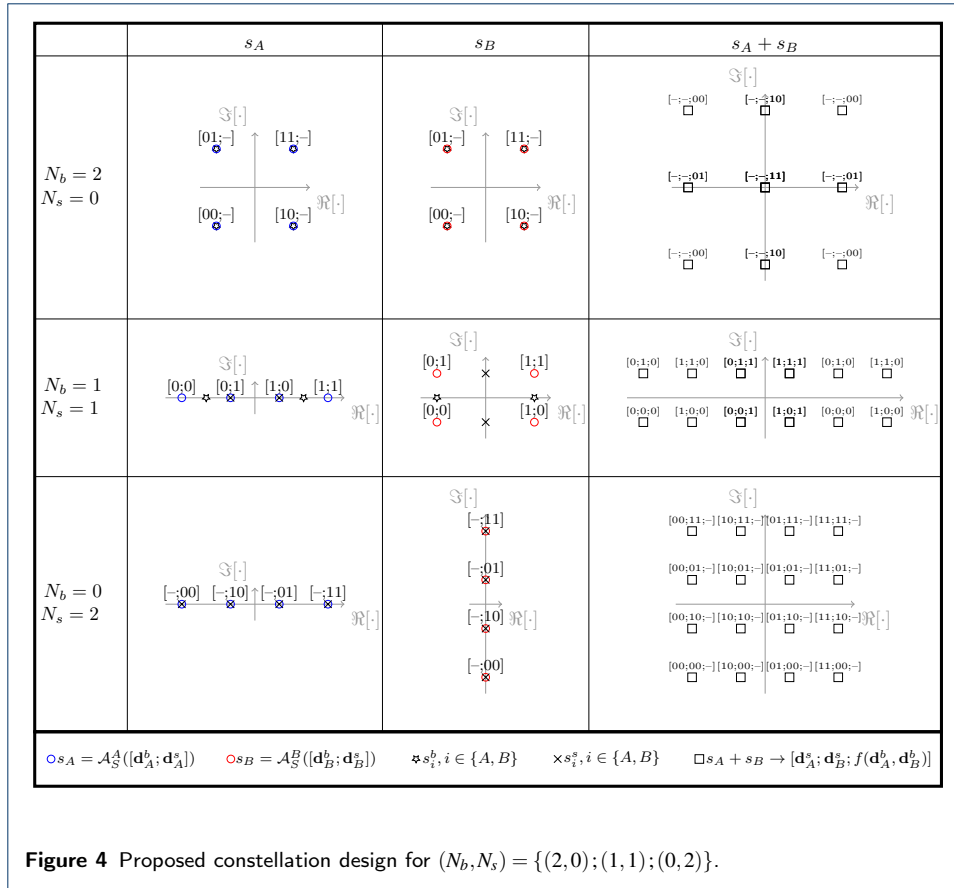
5.85 GHz. In this paper GNURadio [29], which is an open-source tool-kit, is used as the host-processing software.

4.2.1 OFDM Parameters

An OFDM solution is employed with $N_{FFT} = 64$ subcarriers. There are 48 data subcarriers, with a DC carrier, 11 guard carriers and 4 pilot carriers at -21, -7, 7 and 21. A CP of $\frac{1}{4}$, i.e. 16 samples, is employed and a center frequency of $f_c = 2.4$GHz is used. The USRP N210 is limited (by the Gigabit Ethernet link) to support an RF bandwidth up to 25 MHz with 14-bit resolution, though a 1 MHz bandwidth, i.e. 1 MS/s sampling rate, is used here. Each packet contains 16 OFDM symbols of payload with 48 data carriers per symbol and constellation parameters N_b, N_s are set to the desired values. The payload is random data and no channel coding is currently implemented in the system.
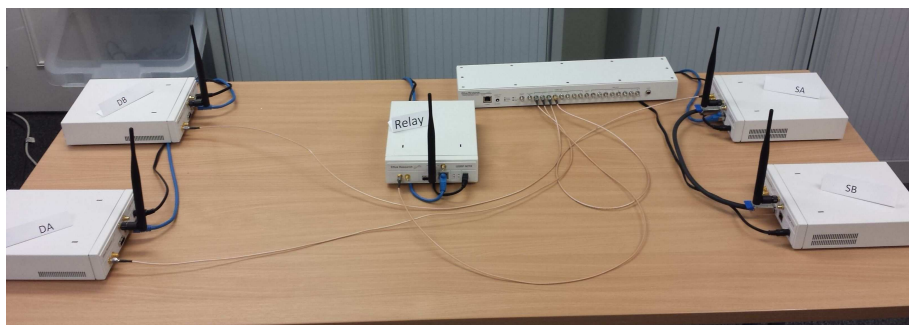
Figure 5 Setup for HW evaluation (Ettus Research USRPs). Source transmissions are prerotated [23–25] to imitate the AWGN channel conditions (as used in the numerical evaluation). To allow a strict control of HSI channels SNR in the HW setup, the HSI channels are emulated by adding a Gaussian noise to the respective source signal and the resulting emulated HSI is passed to destinations via UDP. This also avoids the problem of node visibility where direct links $S_A \rightarrow D_A$ and $S_B \rightarrow D_B$ exist in the laboratory environment.

4.2.2 Node Placement, Synchronization and Channel Estimation

A 5-node, 2x1x2 topology with two sources, one relay and two destinations, is used as shown in Fig. 5. The USRPs each have a single 3dBi omni-directional antenna (at 2.4 - 2.5 GHz and 4.9 - 5.85 GHz). The first source transmitter (S_A) USRP is connected to a powerful Core i7 laptop, running a single instance of GNURadio, by a Gigabit Ethernet link. The second source transmitter (S_B) USRP is connected to the first by the MIMO expansion cable. This provides the second transmitter with baseband data from GNURadio as well as synchronization signals from the first transmitter. The relay, D_A and D_B USRPs are connected to further laptops running GNURadio by Gigabit Ethernet links. More details about synchronization, carrier frequency offset and timing offset estimation can be found in [30]. In this paper, the MIMO cable is used to synchronize the frequency of the two source USRPs, as well as to achieve sample-level timing synchronization. The latter avoids asynchronism in the superimposed constellations at the relays; more details about the impact of asynchronism in WNC can be found in [31]. Furthermore an Ettus Octoclock clock distribution system [32] is used to provide external frequency synchronization signals to all nodes. This allows us to show system performance, and compare with the theoretical and simulation cases, without the impact of asynchronism affecting the results. Results

with additional real-world impairments are a focus for future work, as discussed in the final section of this paper. Channel tracking using pilots is implemented as detailed in [30], however, due to the static indoor environment (used to mimic the AWGN channel used in the theoretical work as closely as possible) the channel does not change significantly over the frame duration. The USRPs are closely located in line-of-sight to ensure the channel between them is fairly static, without fading, thus mimicking the channel used in the theoretical work. Moreover as cabled synchronisation is used, it is desirable to minimize the cable length. Low SNRs are achieved between the USRPs using low transmit powers.

4.3 Uncoded System Throughput

To analyze the performance of the proposed constellations, we evaluate the throughput for fixed γ_{MAC} and γ_{BC} as a function of γ_{HSI}. We analyze all permissible constellations for a fixed $N_b + N_s = 2$ (see Fig. 4) and compare their performance with the throughput T_{ref} of the *reference* "conventional" multi-user detection with regular QAM constellation. Note again that the hierarchical function is set to the bit-wise XOR, i.e. $f\left(\mathbf{d}_A^b, \mathbf{d}_B^b\right) = \mathbf{d}_A^b \oplus \mathbf{d}_B^b$ in the evaluations.

In addition to the analytically evaluated throughput (lower-bound) T_{LB} (9) we also include the result of a numerical Monte-Carlo evaluation of throughput (T_{sim}) over 10^4 frames (Figs. 6, 7, 8, 9) and throughput T_{USRP} evaluated by the HW real world setup (Figs. 8, 9). The particular related assumptions employed in the evaluations are summarized in Table 2 to improve the reader's perception. One can see that the reference scenario with conventional QPSK (4-QAM) provides zero throughput (T_{ref}) in the whole range of analyzed SNRs in all plots[5]. The performance of conventional WNC (in the specific 4-ary case the conventional WNC constellations are identical to $(N_b, N_s) = (2,0)$ [4]) is, on the other hand, inevitably limited to high γ_{HSI} regions in WBN as it requires perfect HSI to enable the decoding of WNC functions at the destination nodes [15]. Remarkably, the novel proposed constellations provide a *non-zero throughput* even in the *low-to-medium SNR* region of

---

[5]In AWGN channel, the resulting superimposed constellation has too many overlaps for the reference source QPSK constellations, preventing a successful multi-user decoding of both of the separate user data streams in the uncoded system.
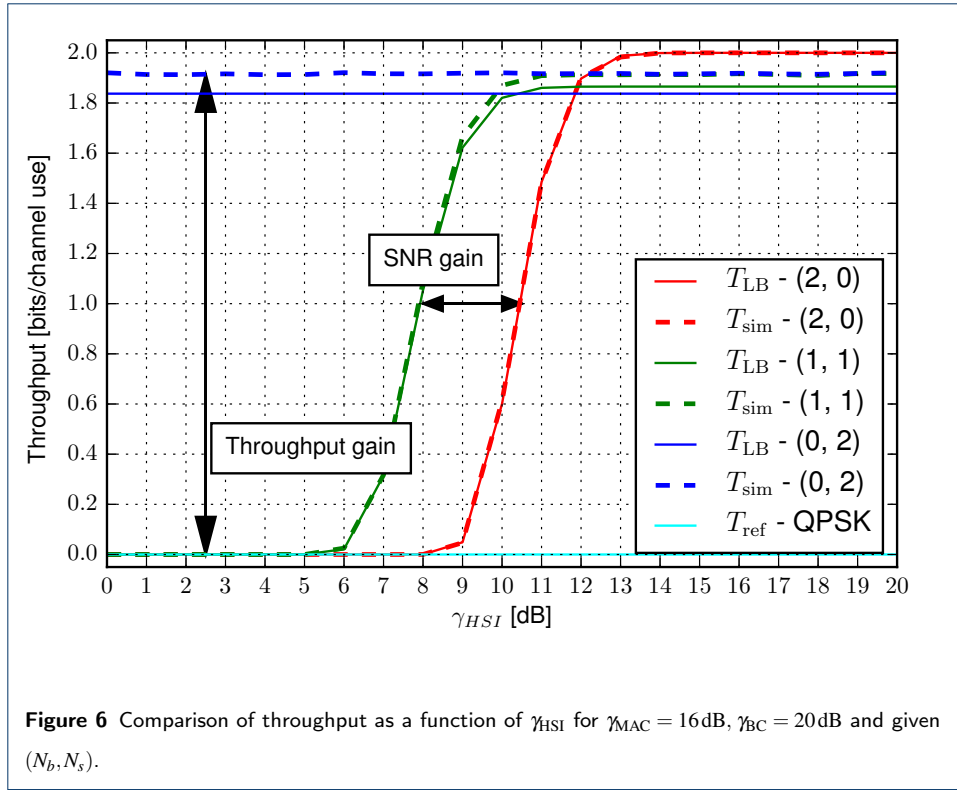
	T_{LB}	T_{sim}	T_{USRP}
Communication channel	AWGN	AWGN	Wireless channel
Time synchronization	Perfect	Perfect	External (Octoclock)
Phase pre-rotation	Perfect	Perfect	Feedback channel (UDP)
Direct link	Not considered	Not considered	Bridged by cable
Channel symmetry	Perfect	Perfect	Node placement
Throughput evaluation	Lower bound	Numerical	Numerical

Table 2 Summary of assumptions in the uncoded system analysis.

HSI channels. The resulting SNR and throughput gains are highlighted in Figs. 6, 7, 8, 9. Note also extremely close agreement of HW performance evaluation T_{USRP} in all cases (Figs. 8, 9). Even in this simple case ($N_b + N_s$ fixed to 2) there are several interesting phenomena which can be observed in the throughput performance:

- The constellations with ($N_b = 0, N_s > 0$) assume full multi-user detection at the relay and hence they do not exploit the HSI channels (Table 1). Consequently, their throughput does not depend on γ_{HSI}. However, their performance worsens with decreasing γ_{MAC} (compare Figs. 8, 6) and deteriorates quite dramatically with decreasing γ_{BC} (compare Figs. 8, 9).

- The constellations with ($N_b > 0, N_s = 0$) require a reliable HSI channel and hence their throughput is zero for low γ_{HSI} and grows up to N_b for high γ_{HSI} and sufficiently high $\gamma_{\text{MAC}}, \gamma_{\text{BC}}$ (all Figs. 6, 7, 8, 9).

- The performance of all constellations with ($N_b > 0, N_s > 0$) is influenced by all system SNRs ($\gamma_{\text{MAC}}, \gamma_{\text{BC}}, \gamma_{\text{HSI}}$). Remarkably, for some particular values of $\gamma_{\text{MAC}}, \gamma_{\text{BC}}$ these constellations significantly outperform those with $N_b = 0$ or $N_s = 0$ in the medium γ_{HSI} region (Figs. 7, 9). Note that this is a direct consequence of superior ρ_{HSI}^2 performance of these constellations[6] for constant $N_b + N_s$, i.e. for constant bits/constellation symbol transmitted by the sources.

---

[6]It can be shown that for constant $N_b + N_s$ the minimum Euclidean distance ρ_{HSI}^2 grows with decreasing N_b, resulting in a more efficient utilization of "imperfect" HSI channels [15, 33] and consequently in a more reliable overheard HSI for the constellations with lower (non-zero) N_b.

Figure 6 Comparison of throughput as a function of γ_{HSI} for $\gamma_{\text{MAC}} = 16\,\text{dB}$, $\gamma_{\text{BC}} = 20\,\text{dB}$ and given (N_b, N_s).
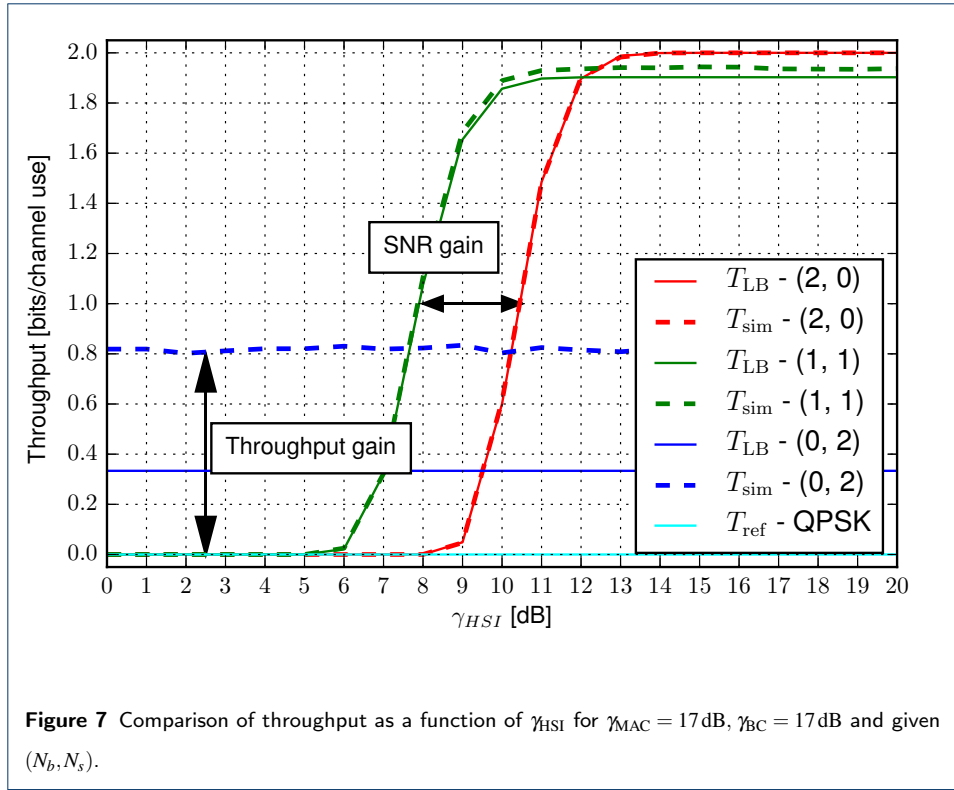
5 Adaptive Constellation Design

As discussed in the previous section, the throughput of the system depends heavily on the actual SNR conditions (given by $\gamma_{\text{MAC}}, \gamma_{\text{BC}}, \gamma_{\text{HSI}}$). By itself, this observation calls naturally for an *adaptive constellation design*. To generate a multi-source constellation able to *maximize the throughput* given the current SNR conditions in the WBN system, the source nodes S_A, S_B must be acquainted with the particular mapping operation $(\hat{\gamma}_{\text{MAC}}, \hat{\gamma}_{\text{BC}}, \hat{\gamma}_{\text{HSI}}) \mapsto (N_b^{\text{I}}, N_s^{\text{I}})$, providing the constellation parameters $N_b^{\text{I}}, N_s^{\text{I}}$ (input arguments to the Algorithm 1) for the given (available) SNR estimates[7] ($\hat{\gamma}_{\text{MAC}}, \hat{\gamma}_{\text{BC}}, \hat{\gamma}_{\text{HSI}}$). The desired *SNR mapping regions* (a three-dimensional look-up table in WBN) can be generated numerically in advance and stored at both source nodes to enable the adaptive constellation mapping.

---

[7]The estimated SNR parameters ($\hat{\gamma}_{\text{MAC}}, \hat{\gamma}_{\text{BC}}, \hat{\gamma}_{\text{HSI}}$) must be delivered to both sources by a feedback channel from the relay and/or destinations. The particular implementation of this feedback transmission is beyond the scope of this paper and hence (for the sake of simplicity) we assume that these parameters are made available at both sources by a genie. Note that in the HW evaluation, the required feedback is provided via UDP connection.

Figure 7 Comparison of throughput as a function of γ_{HSI} for $\gamma_{MAC} = 17\,dB$, $\gamma_{BC} = 17\,dB$ and given (N_b, N_s).
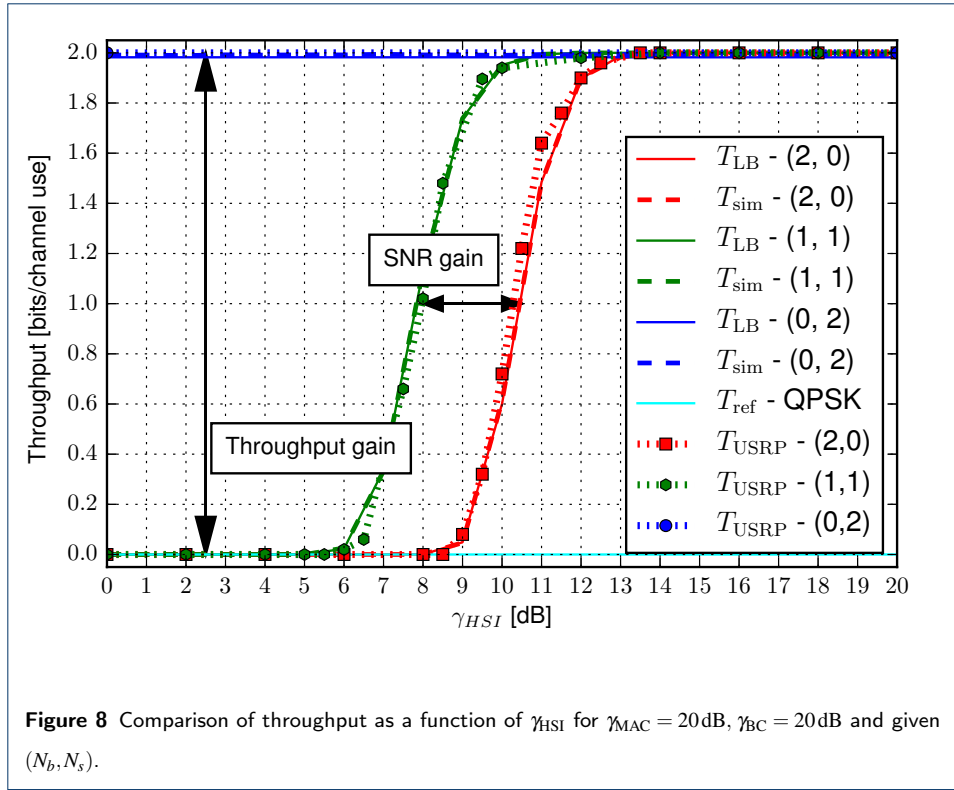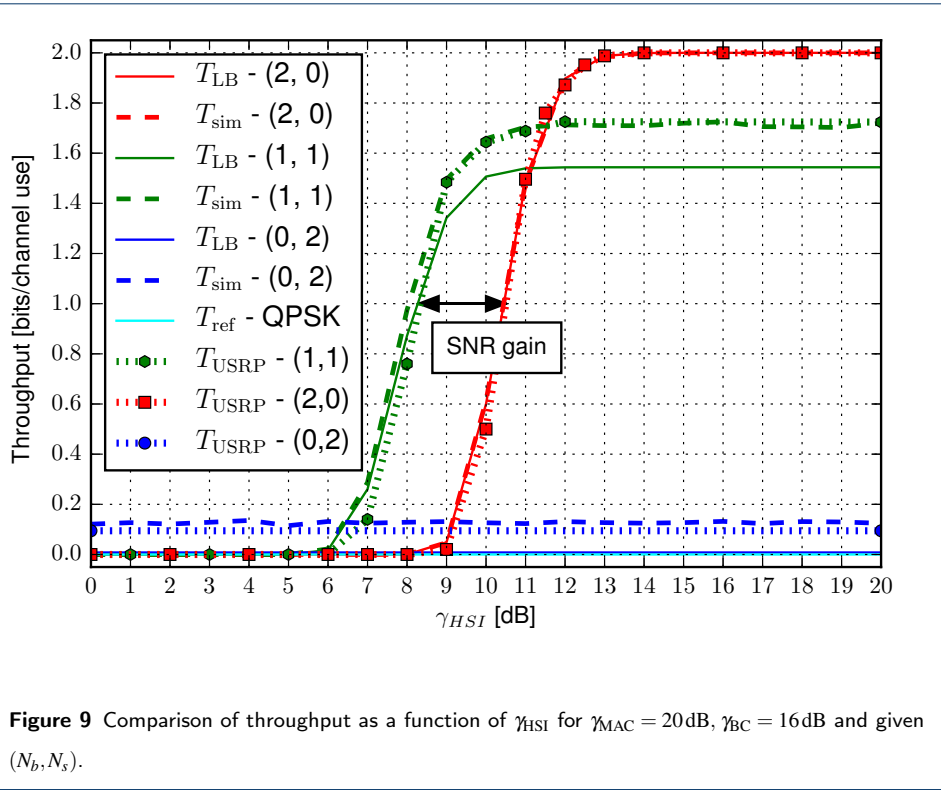
Due to the numerical complexity of Monte-Carlo evaluation of throughput T_{sim} we use the analytically evaluated lower bound T_{LB} (9) to generate the SNR mapping regions for a wide range of γ_{MAC}, γ_{BC}, γ_{HSI}. The optimal constellation parameters (maximizing the throughput T_{LB} for a given SNR triplet γ_{MAC}, γ_{BC}, γ_{HSI}) are found by performing an exhaustive search over the constellation parameters as $(N_b^I, N_s^I) = \arg\max_{(N_b, N_s)} T_{LB}(\gamma_{MAC}, \gamma_{BC}, \gamma_{HSI})$.

The SNR mapping regions, including the resulting throughput for the optimal choice of N_b^I, N_s^I, are shown as a function of γ_{MAC}, γ_{HSI} for $\gamma_{BC} \in \{15\,dB, 17\,dB, 20\,dB, 25\,dB\}$ in Fig. 10. Several interesting phenomenas can be again observed in the figure:

- Since the transmission schemes with $(N_b = 0, N_s > 0)$ constellations can ignore the HSI channels (Table 1), these constellations are optimal in the low γ_{HSI} region ($\gamma_{HSI} < 8\,dB$), regardless of the other channels' SNRs γ_{MAC}, γ_{BC}.

- The constellations with $(N_b > 0, N_s = 0)$ provide the best performance in a substantial part of the medium-to-high γ_{HSI} regions, depending on the actual γ_{MAC}, γ_{BC}.

Figure 8 Comparison of throughput as a function of γ_{HSI} for $\gamma_{MAC} = 20\,\mathrm{dB}$, $\gamma_{BC} = 20\,\mathrm{dB}$ and given (N_b, N_s).

- The "combined" constellations ($N_b > 0, N_s > 0$) provide the maximal throughput (for sufficiently high γ_{BC}) in relatively large regions of γ_{MAC}, γ_{HSI} (see the dominant throughput regions of $(N_b^I, N_s^I) = (2, 1)$ for $\gamma_{BC} = \{20\,\mathrm{dB}, 25\,\mathrm{dB}\}$). Note that these constellations have a great potential for application in systems with limited or partial HSI (see [15]).

- The BC channel SNR (γ_{BC}) can significantly limit the performance of the system, even in the case where both γ_{MAC}, γ_{HSI} are relatively high (compare the results for $\gamma_{BC} = 15\,\mathrm{dB}$ and $\gamma_{BC} = 20\,\mathrm{dB}$ for $\gamma_{MAC} = \gamma_{HSI} \gtrsim 15\,\mathrm{dB}$). This behavior originates in the fact that ρ_{BC}^2 decreases with growing $N_b + 2N_s$ and hence low γ_{BC} essentially limits the maximum efficiently applicable cardinality of the relay output ($2^{N_b + 2N_s}$-QAM) constellation. Equivalently, the optimal source constellation parameters (N_b^I, N_s^I) can become limited by the bottleneck induced by weak relay$\rightarrow$destination (BC) channels.

Figure 9 Comparison of throughput as a function of γ_{HSI} for $\gamma_{\text{MAC}} = 20\,\text{dB}$, $\gamma_{\text{BC}} = 16\,\text{dB}$ and given (N_b, N_s).

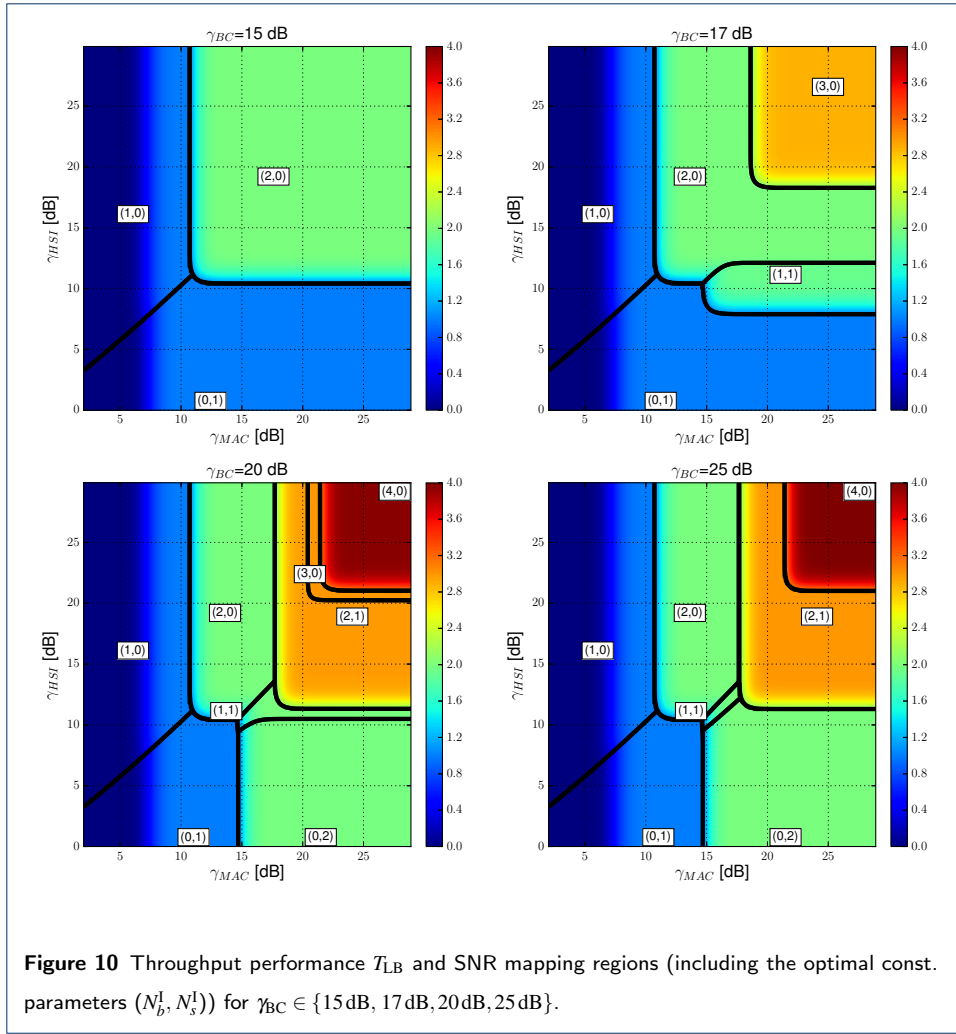- The constellations with odd N_b are rarely dominant over the other strategies with identical $N_b + N_s$. This is a direct consequence of their relatively poor ρ_{MAC}^2 Euclidean distance properties.

To support a viability of the adaptive constellation mapping scheme, we again evaluate the system performance in the HW real world setup. Since the HW evaluation is heavily time-consuming, we analyze the throughput T_{USRP} only for $\gamma_{\text{BC}} = 20\,\text{dB}$ and $0\,\text{dB} \leq \gamma_{\text{MAC}}, \gamma_{\text{HSI}} \leq 30\,\text{dB}$ with a step-size $3\,\text{dB}$. The measured T_{USRP} performance is available in Fig. 11. Close agreement between the T_{USRP} and T_{LB} can be observed again in the whole range of analyzed $\gamma_{\text{MAC}}, \gamma_{\text{HSI}}$ (see Fig. 11).
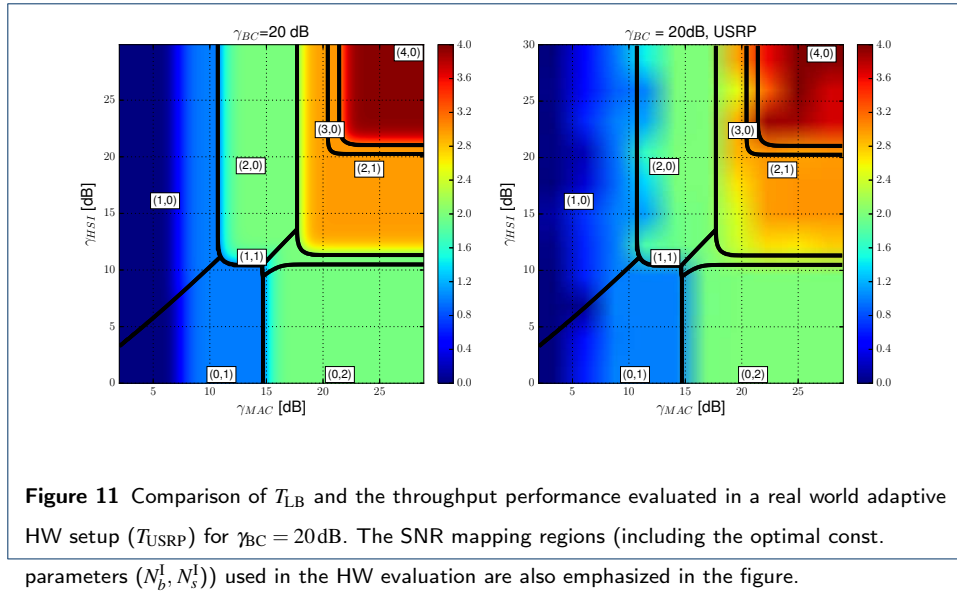
6 Channel Coding

We have shown that Algorithm 1 is a strong tool for the design of source constellations suitable for arbitrary channel SNRs in the WBN system. However, even though the proposed constellations provide promising performance in the uncoded scenario, the extension to a coded system is desirable for practical wireless applications.

Figure 10 Throughput performance T_{LB} and SNR mapping regions (including the optimal const. parameters $(N_b^{\text{I}}, N_s^{\text{I}})$) for $\gamma_{\text{BC}} \in \{15\,\text{dB}, 17\,\text{dB}, 20\,\text{dB}, 25\,\text{dB}\}$.

Considering the communication in uncoded WBNs (Fig. 2), there are many ways to improve its reliability through channel coding. In this paper we propose one particular solution, based on the assumption that each source node splits its data into the basic and superposed part and then encodes these parts separately by two constituent channel encoders[8]. We believe that this approach provides the best insight into the channel-coding extension of WBN systems and hence we focus on its development in the rest of this section.

---

[8]In a more general approach, each source data word is split into $N_b + N_s$ parallel data sub-words that are encoded separately using the principles of multilevel coding (see e.g. [34]). However, the development of a general multilevel coding scheme for WBN is beyond the scope of this paper.

Figure 11 Comparison of T_{LB} and the throughput performance evaluated in a real world adaptive HW setup (T_{USRP}) for $\gamma_{\mathrm{BC}} = 20\,\mathrm{dB}$. The SNR mapping regions (including the optimal const. parameters $(N_b^{\mathrm{I}}, N_s^{\mathrm{I}})$) used in the HW evaluation are also emphasized in the figure.

6.1 Per-link Channel Coding Scheme for Symmetric WBN with Superposition Modulations

In general, it is desirable to protect *all individual transmissions* in the system with error correction coding[9]. Accordingly, the relay node has to decode the desired data (including the particular WNC function) from its observation and then it should perform an additional re-encoding in order to protect the subsequent relay→destinations transmission. The resulting channel coding scheme (see Fig. 12) is introduced in the following text.

6.1.1 Source processing

Source S_A (likewise for S_B) wants to transmit a binary data word $\mathbf{D}_A$ of length $|\mathbf{D}_A| = |\mathbf{D}_B| = k_{\mathbf{D}}$ to its respective destination D_A. Each data word $\mathbf{D}_A$ is split into the basic and superposed part (similarly as in the uncoded case), i.e.:

$$\mathbf{D}_A = [\mathbf{D}_A^b, \mathbf{D}_A^s] = [d_{A,0}^b, d_{A,1}^b, \ldots d_{A,k_{\mathbf{D}}^b-1}^b, d_{A,0}^s, d_{A,1}^s, \ldots d_{A,k_{\mathbf{D}}^s-1}^s],$$

---

[9]Alternatively, a primitive end-to-end coding scheme can be designed, performing the channel coding solely at sources S_A, S_B and channel decoding (potentially computationally intensive) solely at destinations D_A, D_B, while leaving the relay R to operate on a symbol-by-symbol basis (as in the uncoded system). Unfortunately, this approach is only sub-optimal, as in this case the particular transmissions on source→relay and relay→destination channels are not individually protected by channel coding.

where $d_{A,n}^b, d_{A,n}^s \in \{0,1\}$ and $k_{\mathbf{D}}^b, k_{\mathbf{D}}^s$ are the lengths of the basic and superposed data sub-words $\mathbf{D}_A^b, \mathbf{D}_A^s$ (respectively).

Subsequently, individual $\mathbf{D}_A^b, \mathbf{D}_A^s$ are encoded by two separate linear binary encoders $\mathscr{C}_b(\textbf{.}), \mathscr{C}_s(\textbf{.})$ (assumed identical at both sources), producing the constituent codewords as:

$$\mathscr{C}_b(\mathbf{D}_A^b) = \mathbf{C}_A^b = [\mathbf{c}_{A,0}^b, \mathbf{c}_{A,1}^b, \dots, \mathbf{c}_{A,\mathcal{N}-1}^b], \tag{10}$$

$$\mathscr{C}_s(\mathbf{D}_A^s) = \mathbf{C}_A^s = [\mathbf{c}_{A,0}^s, \mathbf{c}_{A,1}^s, \dots, \mathbf{c}_{A,\mathcal{N}-1}^s], \tag{11}$$

where $\mathcal{N}$ is the number of codeword symbols (equivalently the number of channel uses required to transmit the codeword) and

$$\mathbf{c}_{A,j}^b = [c_{A,j_0}^b, \dots, c_{A,j_{N_b}-1}^b],$$

$$\mathbf{c}_{A,j}^s = [c_{A,j_0}^s, \dots, c_{A,j_{N_s}-1}^s]$$

are codeword symbols of length N_b (respectively N_s) bits. The dimensionality of binary codewords is thus $\left|\mathbf{C}_A^b\right| = \left|\mathbf{C}_B^b\right| = n_{\mathbf{C}}^b = \mathcal{N} \cdot N_b$, $\left|\mathbf{C}_A^s\right| = \left|\mathbf{C}_B^s\right| = n_{\mathbf{C}}^s = \mathcal{N} \cdot N_s$.

The constituent codewords $\mathbf{C}_A^b, \mathbf{C}_A^s$ are then forwarded to the joint constellation mapper $\mathscr{A}^A(\textbf{.})$ (provided by Algorithm 1), which produces a sequence of $(N_s + N_b)$-bit constellation symbols $s_{A,j} = \mathscr{A}^A\left(\left[\mathbf{c}_{A,j}^b; \mathbf{c}_{A,j}^s\right]\right)$. Note that in the encoded system it is the codeword symbols that are mapped to the desired constellation (instead of data symbols), but since $\left|\mathbf{c}_A^b\right| = \left|\mathbf{c}_B^b\right| = N_b$ and $\left|\mathbf{c}_A^s\right| = \left|\mathbf{c}_B^s\right| = N_s$, it is sufficient to formally substitute the codeword symbol $\mathbf{c}_i = \left[\mathbf{c}_i^b; \mathbf{c}_i^s\right]$ for the data symbol $\mathbf{d}_i = \left[\mathbf{d}_i^b; \mathbf{d}_i^s\right]$ in Algorithm 1 (lines 10, 15). The resulting constellation symbols are successively transmitted by S_A (simultaneously with $s_{B,j}$ from S_B) towards the relay node.

6.1.2 Relay processing

The crucial part of the encoded WBN system processing is based at the relay node. Like the uncoded case, the relay must decode jointly the *superposed* data sub-words $(\mathbf{D}_A^s, \mathbf{D}_B^s)$ along with the *WNC function* of *basic* data sub-words $(f(\mathbf{D}_A^b, \mathbf{D}_B^b) = \mathbf{D}_A^b \oplus \mathbf{D}_B^b)$. Whilst both $\mathbf{D}_A^s$, $\mathbf{D}_B^s$ can be decoded straightforwardly by the relay (using conventional single user decoders $\mathscr{C}_s^{-1}$), the fundamental question is how to decode the WNC function $f(\mathbf{D}_A^b, \mathbf{D}_B^b)$ since both $\mathbf{D}_A^b$, $\mathbf{D}_B^b$ are encoded separately at sources S_A, S_B[10]. Fortunately, as proven in [13], the WNC function $f(\mathbf{D}_A^b, \mathbf{D}_B^b)$ can be decoded directly from the relay observation (5), if the particular source data words are encoded by the same linear encoder $\mathscr{C}_b$, since

$$
\begin{aligned}
\mathscr{C}_b\left(f(\mathbf{D}_A^b, \mathbf{D}_B^b)\right) &= \mathscr{C}_b\left(\mathbf{D}_A^b \oplus \mathbf{D}_B^b\right) \\
&= \mathscr{C}_b(\mathbf{D}_A^b) \oplus \mathscr{C}_b(\mathbf{D}_B^b) \\
&= \mathbf{C}_A^b \oplus \mathbf{C}_B^b,
\end{aligned}
\tag{12}
$$

where $\mathbf{C}_A^b \oplus \mathbf{C}_B^b$ itself is again a valid codeword and hence the WNC function $f(\mathbf{D}_A^b, \mathbf{D}_B^b)$ can be decoded directly from the relay observation (using a conventional single user decoder $\mathscr{C}_b^{-1}$).
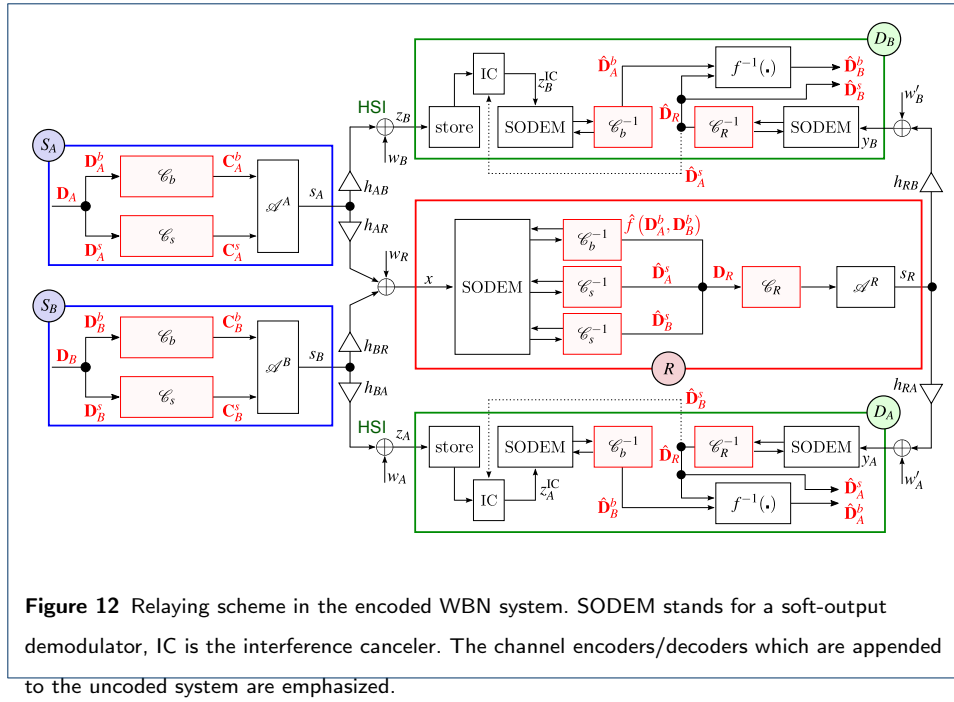
After decoding all required data streams $(\hat{\mathbf{D}}_A^s, \hat{\mathbf{D}}_B^s, \hat{f}(\mathbf{D}_A^b, \mathbf{D}_B^b))$, the relay creates a joint data word $\mathbf{D}_R = [\hat{\mathbf{D}}_A^s, \hat{\mathbf{D}}_B^s, \hat{f}(\mathbf{D}_A^b, \mathbf{D}_B^b)]$ and re-encodes it as $\mathscr{C}_R(\mathbf{D}_R) = \mathbf{C}_R = [\mathbf{c}_{R,0}, \mathbf{c}_{R,1}, \ldots, \mathbf{c}_{R,\mathcal{N}-1}]$. The encoded data are then mapped to the output 2^{N_R}-QAM (where $N_R = 2N_s + N_b$) constellation symbols $s_{R,j} = \mathscr{A}^R(\mathbf{c}_{r,j})$, $j \in \{0, 1, \ldots, \mathcal{N}-1\}$ and broadcast by the relay to both destination nodes.

6.1.3 Destination processing

As in the uncoded case, destinations D_A, D_B firstly store the signal received in the MA phase, and then, after decoding the relay data word $\mathbf{D}_R$ (from the signal received in the BC

---

[10]Note that separate decoding of $\mathbf{D}_A^b$, $\mathbf{D}_B^b$ and subsequent evaluation of $f(\mathbf{D}_A^b, \mathbf{D}_B^b)$ (i.e. conventional joint/multi-user decoding concatenated with traditional network coding [35]) can significantly limit the performance of the system [13].

Figure 12 Relaying scheme in the encoded WBN system. SODEM stands for a soft-output demodulator, IC is the interference canceler. The channel encoders/decoders which are appended to the uncoded system are emphasized.

phase), both destinations can perform IC to remove the unintended superposed codewords from the MA phase signal to get the desired HSI and then finally recover the desired data (see Fig. 12 for the details).

6.2 Analysis of Transmission Rates

The last step in the design of a feasible modulation and coding scheme for WBN (see Fig. 12) is to identify the range of permissible transmission rates for the basic (r_b), superposed (r_s) and relay output (r_R) data streams. To achieve this goal, we analyze the Constellation Constrained (CC) capacities [36] of the proposed source constellations, including the CC capacity of the conventional relay output 2^{N_R}-QAM alphabets (used in the BC phase of communication).

The transmission rates are defined in bits per channel use, and hence $r_i = N_i \cdot k_{\mathbf{D}}^i / n_{\mathbf{C}}^i$, where N_i is the number of bits per channel symbol/use in the data stream i, $i \in \{b, s, R\}$. In accordance with the definition of source and relay codewords, we assume that each communication round requires $2\mathcal{N}$ channel uses, where the length of both MA and BC phase is set to $\mathcal{N}$ channel uses. Note that the assumption that BC and MA phases have identical length is

generally only suboptimal (see e.g. [1, 15]), but nevertheless it is a common assumption in practical systems and hence we limit our attention to this particular case.

6.2.1 Relay observation

After splitting the source data streams, the whole system can be interpreted as a 4-user system where the relay has to decode the data $\mathbf{D}_A^s$, $\mathbf{D}_B^s$, $f(\mathbf{D}_A^b, \mathbf{D}_B^b)$ from the *virtual 3-user* (S_A^s, S_B^s, S_{AB}^b) *multiple-access channel* observation (see Fig. 12). Unfortunately, since one of the users (S_{AB}^b) is only virtual, we cannot simply claim that the region of achievable rates in this virtual channel can be derived directly from the conventional cut-set bound analysis (see e.g. [18, 37]), but rather a careful information-theoretic analysis would be required to identify the exact rate region. However, such analysis is far beyond the scope of this paper, and hence, for simplicity reasons, we only conjecture that the eligible source rates (r_b, r_s) are limited by the conventional CC multiple-access capacity region [18, 37], which can be defined by the following set of mutual informations $I(\cdot; \cdot)$:

$$2r_s + r_b \leq I(x; \mathbf{c}_A^s, \mathbf{c}_B^s, f(\mathbf{c}_A^b, \mathbf{c}_B^b)), \tag{13}$$

$$2r_s \leq I(x; \mathbf{c}_A^s, \mathbf{c}_B^s | f(\mathbf{c}_A^b, \mathbf{c}_B^b)), \tag{14}$$

$$r_s + r_b \leq I(x; \mathbf{c}_A^s, f(\mathbf{c}_A^b, \mathbf{c}_B^b) | \mathbf{c}_B^s), \tag{15}$$

$$r_s + r_b \leq I(x; \mathbf{c}_B^s, f(\mathbf{c}_A^b, \mathbf{c}_B^b) | \mathbf{c}_A^s), \tag{16}$$

$$r_s \leq I(x; \mathbf{c}_A^s | \mathbf{c}_B^s, f(\mathbf{c}_A^b, \mathbf{c}_B^b)), \tag{17}$$

$$r_s \leq I(x; \mathbf{c}_B^s | \mathbf{c}_A^s, f(\mathbf{c}_A^b, \mathbf{c}_B^b)), \tag{18}$$

$$r_b \leq I(x; f(\mathbf{c}_A^b, \mathbf{c}_B^b) | \mathbf{c}_A^s, \mathbf{c}_B^s), \tag{19}$$

where (13), (14)-(16) and (17)-(19) are the corresponding third, second and first order cut-set bounds (respectively). As we show later, the CC MAC region (as defined by (13)-(21)) provides a reasonable estimate of the maximal achievable source transmission rate pair (r_b, r_s) in WBN.

Since the superposed data sub-words $\mathbf{D}_A^s, \mathbf{D}_B^s$ are mapped to orthogonal ASK sets (Algorithm 1), the 2nd order cut-set bound $I(x; \mathbf{c}_A^s, \mathbf{c}_B^s | f(\mathbf{c}_A^b, \mathbf{c}_B^b))$ (14) is equivalent to $I(x; \mathbf{c}_A^s | \mathbf{c}_B^s, f(\mathbf{c}_A^b, \mathbf{c}_B^b)) + I(x; \mathbf{c}_B^s | \mathbf{c}_A^s, f(\mathbf{c}_A^b, \mathbf{c}_B^b))$ (defined in eqs. (17) and (18)), which can be proven easily by the chain rule for mutual information of orthogonal signal sets (see [18]). Moreover, due to the assumed WBN system symmetry, the cut-set bounds defined in equations (17), (18) are identical, and the same is true for the pair of cut-set bounds defined in (15), (16). Consequently, the CC multiple-access capacity region is completely defined by the four inequalities in (13), (15), (17) and (19).

6.2.2 Effective HSI channels

In addition to the successful relay decoding, the transmission rate of the basic information stream r_b must guarantee that the HSI (given by the unintended data sub-words $\mathbf{D}_A^b$ at D_B and $\mathbf{D}_B^b$ at D_A) can be decoded at both destinations (after perfect IC of superposed data codewords $\mathbf{C}_A^s$ at D_B and $\mathbf{C}_B^s$ at D_A from the stored MA phase signal). Note that since we assume that the relay has already successfully decoded $f(\mathbf{D}_A^b, \mathbf{D}_B^b)$ at this step, it can be efficiently exploited in the decoding process, resulting in the following upper-bounds on the source rate r_b:

$$r_b \leq I(z_B^{\text{IC}}; \mathbf{c}_A^b | f(\mathbf{c}_A^b, \mathbf{c}_B^b)), \tag{20}$$

$$r_b \leq I(z_A^{\text{IC}}; \mathbf{c}_B^b | f(\mathbf{c}_A^b, \mathbf{c}_B^b)), \tag{21}$$

where $z_A^{\text{IC}}, z_B^{\text{IC}}$ are the efficient HSI observations (after perfect IC) at D_A, D_B (respectively) – see Fig. 12. Both (20), (21) are identical in the symmetric WBN system.

6.2.3 Relay broadcast channel

The relay rate r_R must guarantee that its data word $\mathbf{D}_R = [\hat{\mathbf{D}}_A^s, \hat{\mathbf{D}}_B^s, \hat{f}(\mathbf{D}_A^b, \mathbf{D}_B^b)]$ with length $|\mathbf{D}_R| = 2k_{\mathbf{D}}^s + k_{\mathbf{D}}^b = \mathcal{N}(2r_s + r_b)$ can be sent to both destinations in $\mathcal{N}$ channel uses. In addition to this, to enable successful decoding of the relay data at both destinations,

the relay transmission rate r_R must be below the CC capacities of the corresponding relay→destination channels. Thus, the relay rate should be set to $r_R = r_b + 2r_s$, which gives us the last two inequalities for r_b, r_s:

$$r_R = 2r_s + r_b \leq I(y_A; \mathbf{c}_R), \tag{22}$$

$$r_R = 2r_s + r_b \leq I(y_B; \mathbf{c}_R), \tag{23}$$

where both cut-set bounds (22), (23) are identical due to the system symmetry.

6.3 Transmission Rate Region for Fixed Source Constellation

To identify the region $(r_b, r_s) \in \mathscr{R}^{(N_b, N_s)}$ of eligible transmission rates for a fixed (N_b, N_s) source constellation, we can evaluate numerically[11] the set of relevant cut-set bounds (i.e. (13), (15), (17), (19), (20) and (22)) for given SNR conditions in the symmetric WBN system (γ_{MAC}, γ_{BC}, γ_{HSI}). An example analysis of the source transmission rate region $\mathscr{R}^{(2,1)}$ for the $(N_b = 2, N_s = 1)$ source constellation is visualized in Fig. 13 for two different SNR setups. The cut-set bound rate region $\mathscr{R}^{(N_b, N_s)}$ is emphasized by the shaded area and the rate pair with maximal $r_b + r_s$ is identified in the figure. We have assumed that the source→relay channels are AWGN (or equivalently that perfect source phase prerotation [23–25] is implemented) in the numerical evaluation.

7 Performance Analysis II: Adaptive Encoded System

As shown in Fig. 13, the performance of the encoded WBN system is, like in the uncoded case, influenced by the immediate SNR conditions (given by γ_{MAC}, γ_{BC}, γ_{HSI}) and hence an *adaptive modulation and coding scheme* is again of interest. However, before we introduce the *SNR mapping operation* for the encoded system, we show that the cut-set bound rate regions $\mathscr{R}^{(N_b, N_s)}$ (as introduced in the preceding section) provide a reasonable approximation of achievable source transmission rate pairs in the symmetric WBN system. In the whole

---

[11]The (conditional) probability density function $p(x|\mathbf{c}_A^s, \mathbf{c}_B^s, f(\mathbf{c}_A^b, \mathbf{c}_B^b))$ which is required for the evaluation of particular mutual information in (13)-(21) can be obtained by a proper marginalization operation $p(x|\mathbf{c}_A^s, \mathbf{c}_B^s, f(\mathbf{c}_A^b, \mathbf{c}_B^b)) = \Pr\{f(\mathbf{c}_A^b, \mathbf{c}_B^b)\} \cdot \sum_{\mathbf{c}_A^b, \mathbf{c}_B^b : f(\mathbf{c}_A^b, \mathbf{c}_B^b)} p(x|\mathbf{c}_A^s, \mathbf{c}_B^s, \mathbf{c}_A^b, \mathbf{c}_B^b)$, where $p(x|\mathbf{c}_A^s, \mathbf{c}_B^s, \mathbf{c}_A^b, \mathbf{c}_B^b)$ is the likelihood function. For more details on the evaluation of CC capacity for finite input constellations see e.g. [13, 37].

section we assume (for simplicity reasons) that perfect source phase prerotation [23–25] is implemented in the system, virtually reverting the source→relay channels to the AWGN case.

7.1 Numerical Simulation of Encoded WBN System Throughput

We implement all constituent channel encoders in the WBN system (see Fig. 12) as parallel concatenated turbo codes with random interleavers of length $\mathcal{N} = 10^5$ symbols. By proper puncturing [38] of the channel encoders' outputs we are able to set the source transmission rates (separately for the basic and superposed streams) to an almost arbitrary value in the range ($^1/_3 \to 1$). We set the initial source transmission rates to the maximum $r_b + r_s \in \mathscr{R}^{(N_b, N_s)}$ (as evaluated in Fig. 13) and by proper adjustment of the puncturing operation we successively decrease the source transmission rates r_b, r_s until the SER performance drops to zero. As one can see in Fig. 13, the achieved transmission rate pairs are relatively close to the maximal permissible values and hence we can consider the cut-set bound rate region $\mathscr{R}^{(N_b, N_s)}$ (as discussed in Section 6.3) to be a reasonable approximation of the achievable source transmission rate region.

7.2 Maximal Throughput of the Adaptive Modulation-Coding Scheme

As in the uncoded case, the source nodes S_A, S_B in the adaptive modulation-coding WBN system must be aware of the particular mapping operation $(\hat{\gamma}_{\mathrm{MAC}}, \hat{\gamma}_{\mathrm{BC}}, \hat{\gamma}_{\mathrm{HSI}}) \mapsto \left(N_b^{\mathrm{II}}, N_s^{\mathrm{II}}; r_b^{\mathrm{II}}, r_s^{\mathrm{II}}\right)$, providing the set of optimal (in the sense of maximal throughput) constellation/encoder parameters for the given SNR conditions $(\hat{\gamma}_{\mathrm{MAC}}, \hat{\gamma}_{\mathrm{BC}}, \hat{\gamma}_{\mathrm{HSI}})$. Note that, in general, all adaptive system parameters are functions of the actual SNR conditions in the system. However, we mostly omit the explicit notation in the following text for to aid readability.

The desired adaptive system parameters can be obtained in the following two-step procedure. First of all, we analyze the cut-set bound rate regions $\mathscr{R}^{(N_b, N_s)}$ (as discussed in Section 6.3) to identify the maximal encoded system throughput $T_C^{(N_b, N_s)}$ for a fixed source

constellation (N_b, N_s):

$$T_C^{(N_b,N_s)}(\gamma_{\text{MAC}}, \gamma_{\text{BC}}, \gamma_{\text{HSI}}) = \max_{r_b, r_s \in \mathscr{R}^{(N_b,N_s)}} (r_b + r_s), \tag{24}$$

$$= r_b^{\max}(N_b, N_s) + r_s^{\max}(N_b, N_s). \tag{25}$$

Then, an exhaustive search over the constellation parameters N_b, N_s can be performed to find the maximum encoded system throughput $T_C^{\max}$ for the given SNR conditions $(\gamma_{\text{MAC}}, \gamma_{\text{BC}}, \gamma_{\text{HSI}})$:

$$T_C^{\max}(\gamma_{\text{MAC}}, \gamma_{\text{BC}}, \gamma_{\text{HSI}}) = T_C^{(N_b^{\text{II}}, N_s^{\text{II}})} = \max_{(N_b,N_s)} T_C^{(N_b,N_s)}, \tag{26}$$

where $(N_b^{\text{II}}, N_s^{\text{II}})$ are the *optimal source constellation parameters*. The corresponding *optimal source transmission rates* (25) are given simply by $r_b^{\text{II}} = r_b^{\max}(N_b^{\text{II}}, N_s^{\text{II}})$, $r_s^{\text{II}} = r_s^{\max}(N_b^{\text{II}}, N_s^{\text{II}})$.

The SNR mapping regions (including the throughput $T_C^{\max}$) for the adaptive modulation and coding scheme in WBN are evaluated as a function of γ_{MAC}, γ_{HSI} in Fig. 14 for $\gamma_{\text{BC}} \in \{7.5\,\text{dB}, 15\,\text{dB}\}$. As one can see in Fig. 15, the increased reliability of transmissions on all individual channels in WBN (as compared to the uncoded system) translates directly into a significant enhancement of throughput performance in the whole range of observed SNRs. This observation justifies the viability of the proposed channel coding scheme.

7.3 Robustness Analysis

In this section we show that the proposed modulation and coding scheme is viable even if the real world conditions induce some deviations from the system model assumed in this paper. From a practical point of view, we would be interested mainly in the situation, where a direct channel between a source and its desired destination is present (see Fig. 16). Even though that this "direct" channel can be relatively weak, it inevitably affects the destinations' HSI observations. In addition to this, we analyse the system where source phase

pre-rotation is switched off (or ineffective due to rapid channel dynamics), and thus the relay faces a multiple-access channel with a varying source channel phase offset. This assumption is valid for a practical system where the applicability of source phase pre-rotation is limited due to the unavailable ideal feedback channel or because of the undesirable delay induced by the feedback in the pre-rotation operation. To demonstrate the robustness of the proposed modulation and coding strategy, we compare the WBN performance results achieved by the Monte-Carlo numerical evaluation (see section 7.1) with USRP HW measurements. While in the numerical evaluation we still keep the idealized assumptions as defined by our system model (i.e. no direct source→destination channels, perfect channel phase pre-rotation), in the HW measurements we now let all data communication to be performed through real wireless channels (compare with the HW setup in section 4.2), introducing inevitably some direct channel observation at both destinations. In addition, we allow the source phase pre-rotation to be switched off in the HW measurements. The channel SNRs $\gamma_{\mathrm{MAC}}, \gamma_{\mathrm{HSI}}$ in the HW measurements can be controlled by the source transmit power adjustment and similarly, particular values of γ_{BC} can be set up by the adjustment of the relay transmit power.

To perform a comparison of the idealized numerical evaluation with the HW robustness measurements, we evaluate the range of SNRs where a zero error rate performance can be achieved for fixed constellations and channel encoder rates (N_b, N_s, r_b, r_s). To achieve this, we identify the triplet of SNRs $(\gamma_{\mathrm{MAC}}, \gamma_{\mathrm{HSI}}, \gamma_{\mathrm{BC}})$ providing a zero-error rate performance at both destinations. This SNR triplet then defines the lower-most corner of the SNR region where a zero error rate performance can be achieved (see Fig. 17). We can conclude that:

- The presence of direct links requires only a slightly increased values of $(\gamma_{\mathrm{MAC}}, \gamma_{\mathrm{HSI}}, \gamma_{\mathrm{BC}})$ to ensure a zero error-rate performance for the fixed (N_B, N_S, r_b, r_s). However, it is evident that a modification of the proposed modulation and coding scheme could be desirable to fully harness the information transmitted over direct source destination channels.

- The source channel phase asynchrony in the system with direct links further degrades the performance on the sources→relay channel and thus an additional increase of the source transmission power (and consequently γ_{MAC}) is required to provide a zero-error rate. However, γ_{BC} is not affected in this case, as the channel pre-rotation does not have any impact on the relay→destination performance.

7.4 Three-Step Reference Scenario

For a more advanced comparison of the proposed method, we consider two conventional *3-step* communication scenarios.

The first scenario is equivalent to a conventional routing, where the sources subsequently transmit their data packet towards the relay. Relay then sends a complete source information (no NC coding is applied) and thus the HSI channels are completely ignored (see Figure 19).

In the second scenario both sources again transmit their information one by one, but the relay is allowed to combine the received (fully decoded) data packets into the network coded packet $f(d_A, d_B) = d_A \oplus d_B$ and HSI channels are necessary to retrieve the desired information at both sources (see Figure 18).

To provide a fair comparison, in both reference scenarios we assume that the sources transmit at double power, as they transmit time is essentially halved when compared with the 2-step scenarios.

We compared throughput of the proposed adaptive constellation design from Section 7.2 on the USRP devices with optimized tuple (r_b, r_s, N_b, N_s) for each measured point (HW-pre-rotation on) with the reference scenarios in Figures 20 and 21. We also considered the proposed method with pre-rotation turned off as in Section 7.3 for comparison. Finally, we added two theoretical limits for the 3-step scenarios, where ideal Gaussian alphabets are assumed.

One can observe that

8 Conclusions and Future Work

In this paper we have proposed a systematic algorithm for the design of two-source constellations in the WBN system. The Algorithm 1 allows the matching of the constellation parameters to virtually any SNR conditions in the system, enabling a direct implementation of the adaptive constellation mapping scheme. The viability of the proposed constellation design was verified by a means of numerical analysis and simulations and also by a real-world HW experiment (based on Ettus Research USRPs), including a HW-based robustness analysis.

Even in the uncoded scenario, the proposed constellations are able to significantly boost the WBN system throughput, and hence even their uncoded implementation can be interesting, especially in some basic wireless networks where channel coding is avoided to reduce complexity (e.g. in sensor networks). Furthermore, we have shown that the proposed source constellation design can be readily extended with appropriately designed channel encoding/decoding operations, significantly improving the reliability (including the throughput) of the resulting adaptive modulation-coding scheme.

In future work, we would like to focus on a full adaptive HW implementation of the proposed system, where the impact of several other parameters (e.g. channel fading and dynamics, asymmetry of channel gains etc.) can significantly affect the system performance and possibly even require some modifications of the adaptive system design.

Nomenclature

ASK	Amplitude Shift Keying
AWGN	Additive White Gaussian Channel
BC	Broadcast Channel
CC	Constellation Constrained
CP	Cyclic Prefix
DC	Direct Current
DEM	Demodulator
FER	Frame Error Rate
HSI	Hierarchical Side Information
HW	Hardware
IC	Interference Cancellation
MA	Multiple Access

MAC	Multiple Access Channel
MIMO	Multiple Input Multiple Output
ODFD	Orthogonal Frequency Division Multiplexing
QAM	Quadrature Amplitude Modulation
QPSK	Quadrature Phase Shift Keying
SC	Superposition Coding
SDR	Software Defined Radio
SER	Symbol Error Rate
SNR	Signal to Noise Ratio
SODEM	Soft Output Demodulator
UDP	User Datagram Protocol
UHD	USRP Hardware Driver
USRP	Universal Software Radio Peripherals
WBN	Wireless Butterfly Network
WNC	Wireless Network Coding

Declarations

This work was partly reported in IEEE ICC [11].

Availability of Data and Materials

We are aware that the presented topic is difficult to understand without very specific background in wireless network coding. To help the reader to overcame this problem, we created a short tutorial [17]. The tutorial first motivates the constellation design, then it shortly introduces the wireless network coding principle, its relation to conventional network coding. Many visual demonstrations of the proposed constellation design can be also found there. In addition to this, the supplementary Python code is available to the reader so that one can touch the topic also by means of implemented algorithms.

Author details

[1]Czech Technical University in Prague, Technicka 2, 16627 Prague, CZ. [2]Toshiba − Telecommunication Research Laboratory, 32 Queen Square, BS1 4ND Bristol,, UK.

References

1. Popovski, P., Yomo, H.: Physical network coding in two-way wireless relay channels. In: Proc. IEEE Internat. Conf. on Commun. (ICC) (2007)

2. Nazer, B., Gastpar, M.: Reliable physical layer network coding. Proc. IEEE **99**(3), 438–460 (2011)

3. Zhang, S., Liew, S.-C., Lu, L.: Physical-layer network coding: Tutorial, survey, and beyond. Physical Communication **2012**, 1–39 (2012). doi:10.1016/j.phycom.2012.05.002

4. Koike-Akino, T., Popovski, P., Tarokh, V.: Denoising maps and constellations for wireless network coding in two-way relaying systems. In: Proc. IEEE Global Telecommunications Conf. (GlobeCom) (2008)

5. Liu, J., Tao, M., Xu, Y.: Pseudo exclusive-OR for LDPC coded two-way relay block fading channels. In: Proc. IEEE Internat. Conf. on Commun. (ICC), pp. 1–5 (2011)

6. Yasami, K., Razi, A., Abedi, A.: Analysis of channel estimation error in physical layer network coding. IEEE Commun. Lett. **15**(10), 1029–1031 (2011). doi:10.1109/LCOMM.2011.082011.110301

7. Uricar, T., Sykora, J.: Non-uniform 2-slot constellations for bidirectional relaying in fading channels. IEEE Commun. Lett. **15**(8), 795–797 (2011)

8. Zhang, S., Liew, S.-C., Lam, P.P.: On the synchronization of physical-layer network coding. In: Proc. IEEE Inf. Theory Workshop (ITW), pp. 404–408 (2006)

9. Rossetto, F., Zorzi, M.: On the design of practical asynchronous physical layer network coding. In: Proc. IEEE Workshop on Signal Processing Advances in Wireless Communications, pp. 469–473 (2009)

10. Huang, Y., Wang, S., Song, Q., Guo, L., Jamalipour, A.: Synchronous physical-layer network coding: A feasibility study. IEEE Trans. Wireless Commun. **12**(8) (2013)

11. Prochazka, P., Uricar, T., Halls, D., Sykora, J.: Relaying in butterfly networks: Superposition constellation design for wireless network coding. In: Proc. IEEE Int. Conf. on Commun. (ICC), London, UK, pp. 1–7 (2015)

12. Nazer, B., Gastpar, M.: Compute-and-forward: Harnessing interference with structured codes. In: Proc. IEEE Internat. Symp. on Inf. Theory (ISIT), pp. 772–776 (2008)

13. Sykora, J., Burr, A.: Layered design of hierarchical exclusive codebook and its capacity regions for HDF strategy in parametric wireless 2-WRC. IEEE Trans. Veh. Technol. **60**(7), 3241–3252 (2011)

14. Uricar, T., Qian, B., Sykora, J., Mow, W.H.: Superposition coding for wireless butterfly network with partial network side-information. In: Proc. IEEE Wireless Commun. Network. Conf. (WCNC), Shanghai, China, pp. 1–6 (2013)

15. Uricar, T., Qian, B., Sykora, J., Mow, W.H.: Wireless (physical layer) network coding with limited hierarchical side-information: Maximal sum-rates in 5-node butterfly network. IEEE Trans. Wireless Commun. **13**(10), 5582–5595 (2014)

16. Ho, I.W.-H., Liew, S.C., Lu, L.: Feasibility study of physical-layer network coding in 802.11p VANETs. In: Proc. IEEE Internat. Symp. on Inf. Theory (ISIT), pp. 646–650 (2014). doi:10.1109/ISIT.2014.6874912

17. Prochazka, P.: WNC Tutorial - Constellation Design for Butterfly Network. http://pavel.prochazka.info/tutorial/const_design_WNC. Accessed: 2016-12-28

18. Cover, T.M., Thomas, J.A.: Elements of Information Theory. John Wiley & Sons, The Atrium, Southern Gate, Chichester PO19 8SQ, UK (1991)

19. Han, T.S., Kobayashi, K.: A new achievable rate region for the interference channel. IEEE Trans. Inf. Theory **27**, 49–60 (1981)

20. Shende, N., Rajan, B.S.: On the achievable rate of AWGN relay channel with finite input constellations. In: Proc. National Conference on Communications (NCC), pp. 1–5 (2012)

21. Popovski, P., de Carvalho, E.: Improving the rates in wireless relay systems through superposition coding. IEEE Trans. Wireless Commun. **7**(12), 4831–4836 (2008)

22. Hoeher, P.A., Wo, T.: Superposition modulation: Myth and facts. IEEE Communications Mag. **49**(12), 110–116 (2011)

23. Koike-Akino, T., Popovski, P., Tarokh, V.: Optimized constellations for two-way wireless relaying with physical network coding. IEEE J. Sel. Areas Commun. **27**(5), 773–787 (2009)

24. Zhang, S., Liew, S.-C.: Applying physical-layer network coding in wireless networks. EURASIP J. on Wireless Comm. and Netw. **2010**, 1–12 (2010). doi:10.1155/2010/870268

25. Li, A., Yan, Y., Kayama, H.: An enhanced denoise-and-forward relaying scheme for fading channel with low computational complexity. IEEE Signal Process. Lett. **15** (2008)

26. Hekrdla, M., Sykora, J.: On indexing of lattice-constellations for wireless network coding with modulo-sum decoding. In: Vehicular Technology Conference (VTC Spring), 2013 IEEE 77th, pp. 1–6 (2013)

27. Prochazka, P.: Nonbinary channel coded physical layer network coding over modulo-sum algebraic ring structures. IEEE Commun. Lett. **20**(3), 538–541 (2016)

28. Research, E.: N200/N210 Product overview. https://www.ettus.com/content/files/07495_Ettus_N200-210_DS_Flyer_HR_1.pdf

29. GNURadio: GNURadio overview. http://gnuradio.org/redmine/projects/gnuradio

30. Hynek, T., Halls, D., Sykora, J.: Practical implementation of cloud initialization procedure for wireless physical layer network coding clouds. In: Proc. European Wireless Conf. (EW), pp. 1–6 (2014)

31. Halls, D., Thompson, W., Galimberti, S., Savazzi, S., Hynek, T., Sykora, J., Coon, J.: Evaluation of practical system constraints, DIWINE deliverable D5.12. Technical report, FP7 ICT Objective 1.1 - The Network of the Future (sep 2014)

32. Research, E.: OctoClock-G Product overview. https://www.ettus.com/product/details/OctoClock-G

33. Uricar, T., Sykora, J.: Non-uniform 2-slot constellations for relaying in butterfly network with imperfect side information. IEEE Commun. Lett. **16**(9), 1369–1372 (2012)

34. Wachsmann, U., Fischer, R.F.H., Huber, J.B.: Multilevel codes: theoretical concepts and practical design rules. IEEE Trans. Inf. Theory **45**(5), 1361–1391 (1999)

35. Yeung, R.W., Li, S.-Y.R., Cai, N., Zhang, Z.: Network Coding Theory. NOW Publishers, 2600 AD Delft, The Netherlands (2006)

36. Biglieri, E.: Coding for Wireless Channels. Springer, 233 Spring Street, New York, NY 10013-1578,USA (2010)

37. Harshan, J., Rajan, B.S.: On two-user gaussian multiple access channels with finite input constellations. IEEE Trans. Inf. Theory **57**(3), 1299–1327 (2011)

38. Schlegel, C.B., Perez, L.C.: Trellis and Turbo Coding: Iterative and Graph-Based Error Control Coding. John Wiley & Sons, The Atrium, Southern Gate, Chichester PO19 8SQ, UK (2015)
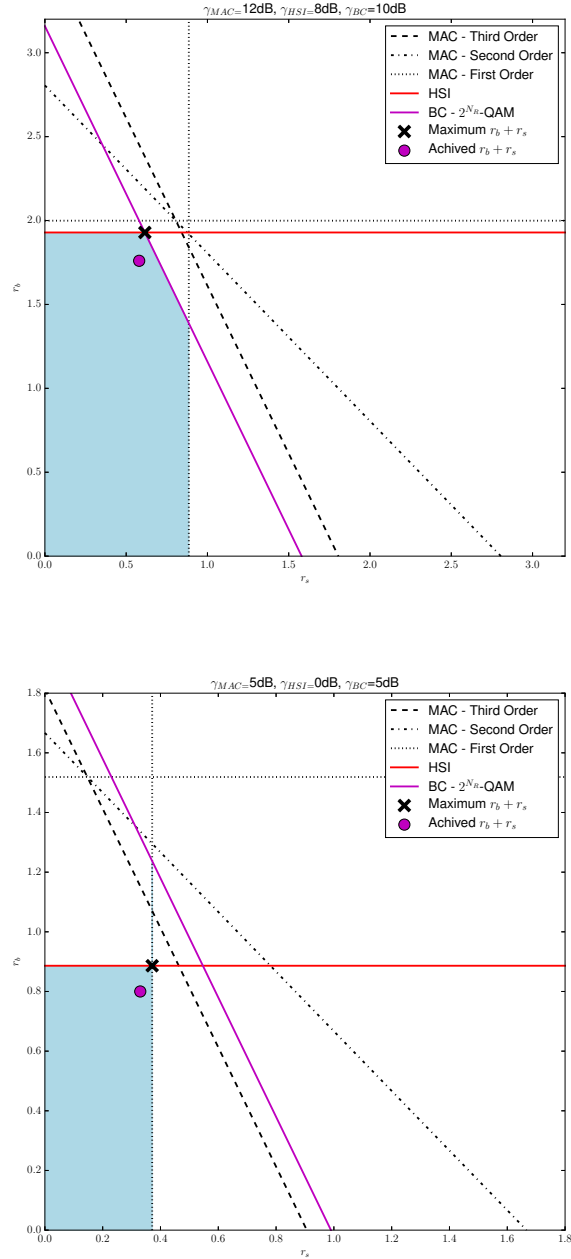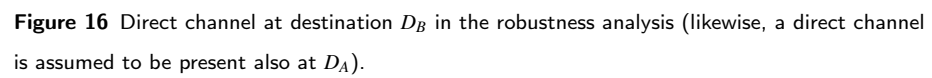
Figure 13 Numerically evaluated cut-set bounds (mutual information for finite input constellations) for $(N_b = 2, N_s = 1)$ source constellations and 16-QAM at the relay. The particular SNR conditions are available in the titles of both sub-figures.
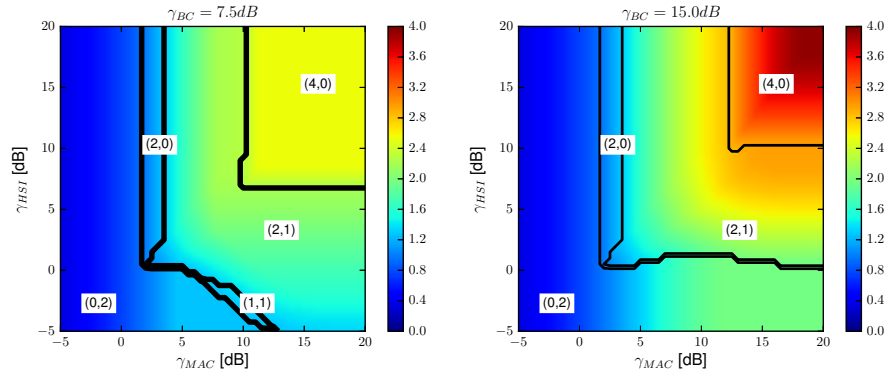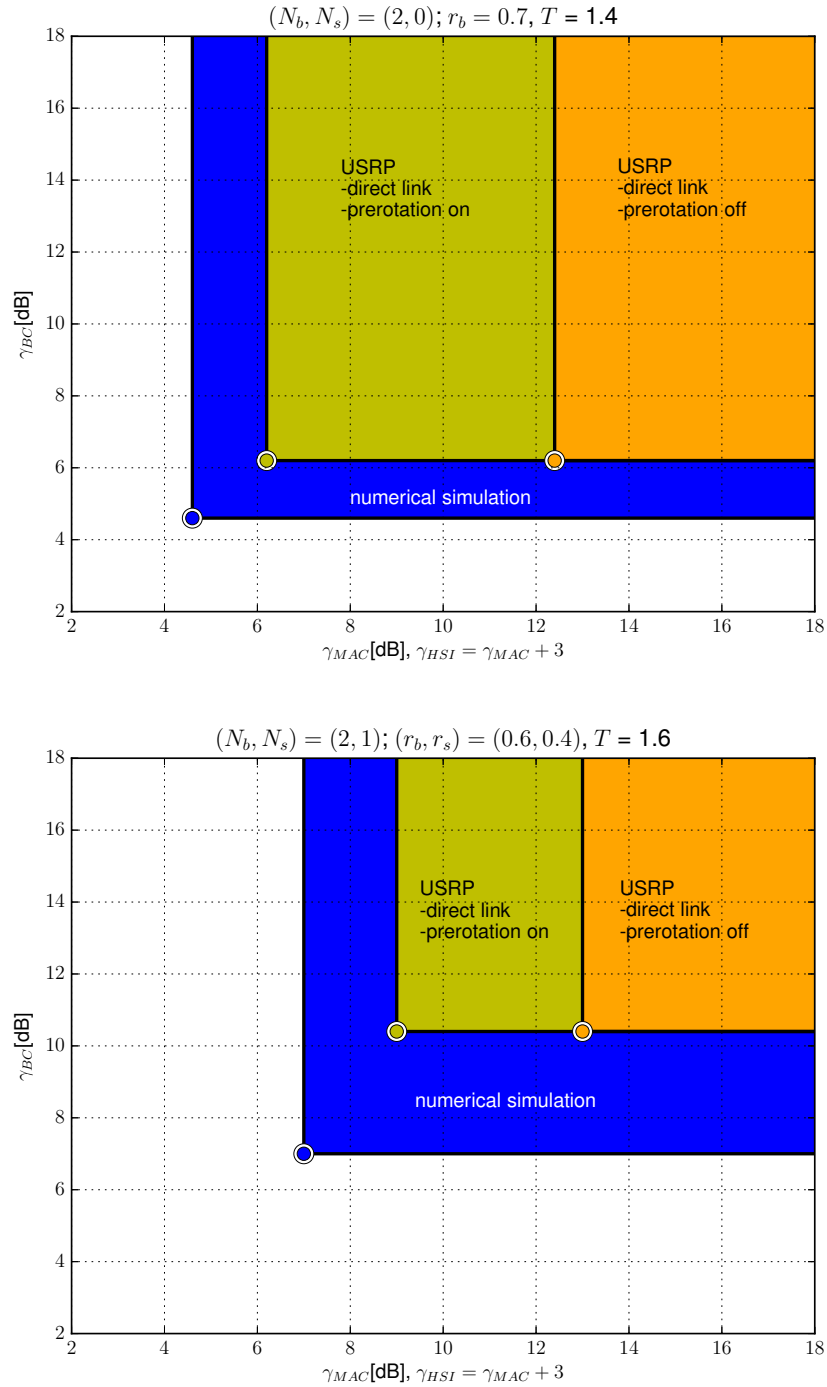
Figure 14 Maximal encoded system throughput $T_C^{\max}$ for $\gamma_{BC} = 7.5\,\text{dB}$ and $\gamma_{BC} = 15\,\text{dB}$.
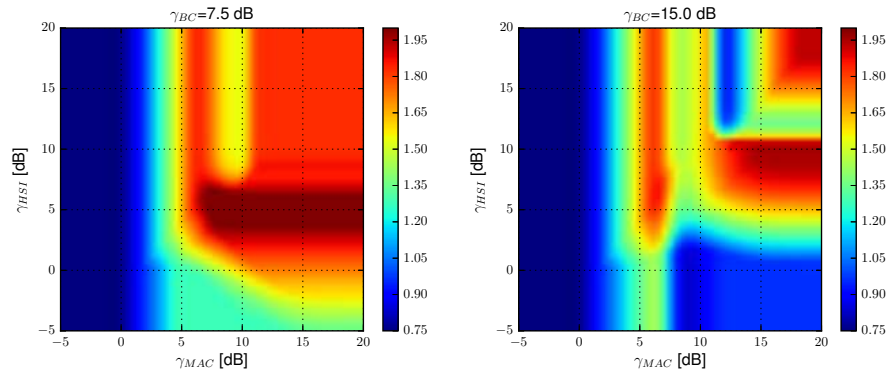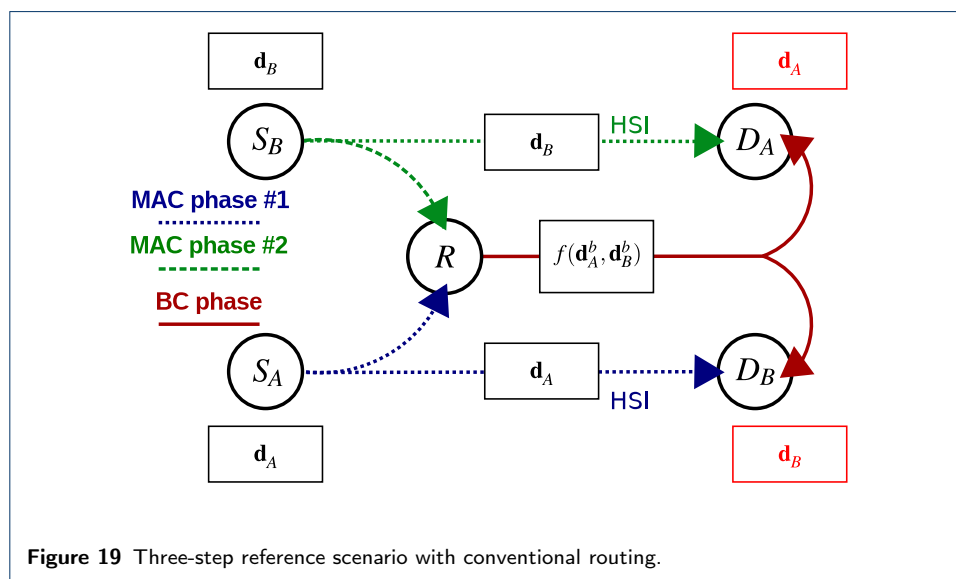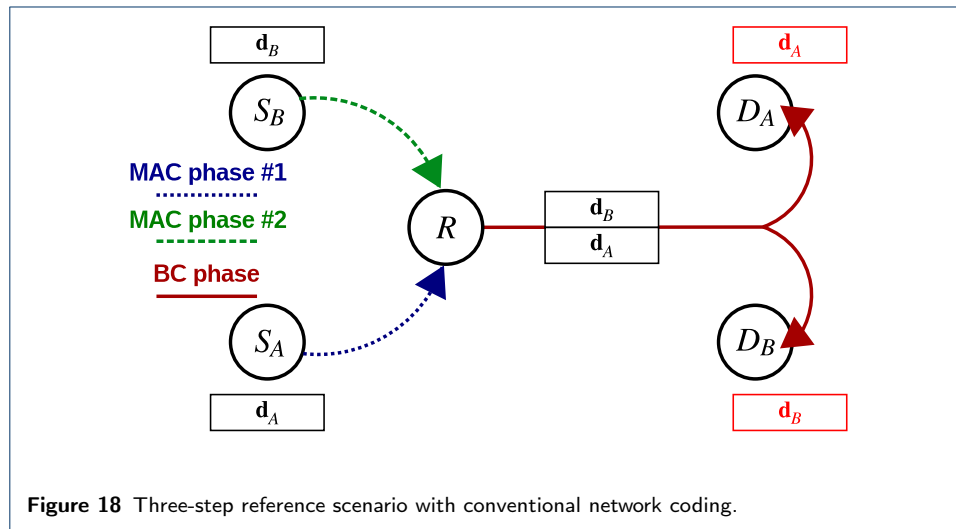

Figure 15 Throughput enhancement $\Delta T_C = T_C^{\max} - T_{LB}$ [bits/channel use] of the coded over uncoded WBN system for $\gamma_{BC} = 7.5\,\text{dB}$ and $\gamma_{BC} = 15\,\text{dB}$. Note that $0.75 \leq \Delta T_C \leq 2$ in the analyzed range of channel SNRs.
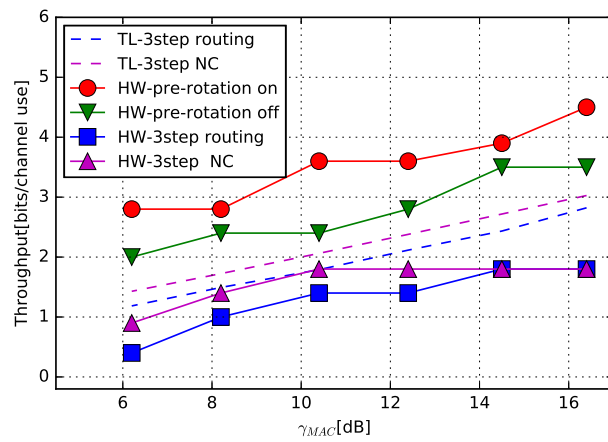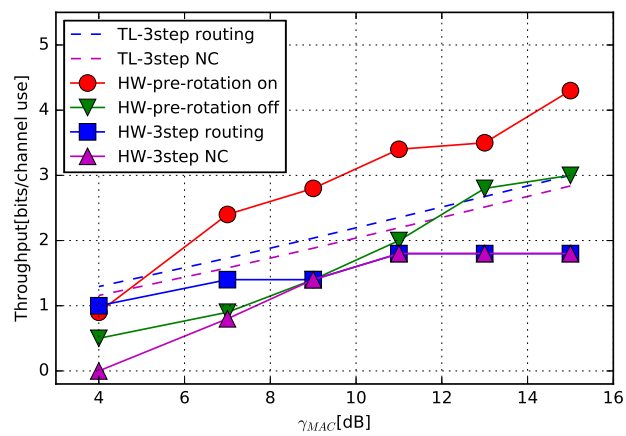
Figure 16 Direct channel at destination D_B in the robustness analysis (likewise, a direct channel is assumed to be present also at D_A).

Figure 17 Robustness analysis for two fixed (N_b, N_s, r_b, r_s) scenarios.

Figure 18 Three-step reference scenario with conventional network coding.

Figure 19 Three-step reference scenario with conventional routing.

Figure 20 Performance comparison for the setup $\gamma_{BC} \approx \gamma_{MAC}$ and $\gamma_{HSI} \approx \gamma_{MAC}+3dB$.

Figure 21 Performance comparison for the setup $\gamma_{BC} \approx \gamma_{MAC}+5dB$ and $\gamma_{HSI} \approx \gamma_{MAC}-1dB$.